A review of the antibiotic ofloxacin: current status of ecotoxicology and scientific advances in its removal from aqueous systems by adsorption technology

Jordana Georgin[1] , Dison Stracke Pfingsten Franco[2], Claudete Gindri Ramos[2],

Daniel G. A. Piccilli[1], Eder C. Lima[3], Farooq Sher[4]

[1-]*Postgraduate Program in Civil Engineering, Federal University of Santa Maria, 97105-900*

Santa Maria, Brazil.

[2-]*Department of Civil and Environmental. Universidad de la Costa, CUC, Calle 58 # 55–66,*

Barranquilla, Atlántico, Colombia.

[3-]*Institute of Chemistry, Federal University of Rio Grande do Sul (UFRGS), Porto Alegre, RS,*
Brazil.

[4-] *Department of Engineering, Nottingham Trent University, Nottingham NG11 8NS, United*
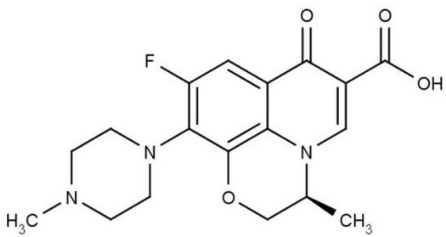*Kingdom*

Abstract

It is estimated that the growth of the population, the augmented expectancy of life, and the emergence of new pandemics will significantly increase the consumption of pharmaceutical drugs in the coming years. Due to its high efficiency, the group of fluoroquinolones, where the antibiotic ofloxacin hydrochloride (OFL) is found, is widely used to combat bacterial infections in humans and animals. The big problem is concentrated in the effluents generated by industries and hospitals. Additionally, most of the drug is not absorbed by the body and is released directly into domestic effluents. On the other hand, treatment stations have removal limitations for small concentrations. This review analyzed all adsorbents developed and used in OFL removal, listing the main parameters influencing the process. In the end, the other existing technologies in the literature and the gaps and future prospects were described. OFL adsorption in most studies occurs under basic conditions (pH between 6.5 and 8). The increase in concentration provides an increase in adsorption capacity. The adsorbents analyzed showed moderate kinetics, reaching equilibrium before 250 min for most studies. The pseudo-second-order model showed the best statistical fit. In most of the studies, the increase in temperature (313, 315, and 328 K) favored the adsorption of OFL. The Langmuir monolayer model represented most of the isothermal studies. The adsorption capacity varied from 3702 to 0.3986 mg g^{-1}. In this aspect, factors such as OFL concentration and textural characteristics of the adsorbent exerted great influence. The thermodynamic parameters were compatible with the isothermal data, where the endothermic nature of the studies was confirmed. Physical interactions (π-π stacking, H bonding, hydrophobic and electrostatic interactions) governed the main adsorption mechanism. Although some studies stated that chemosorption occurred, thermodynamic parameters cannot validate the same. Coexisting ions in the solution can positively and negatively influence OFL adsorption. The listed studies are all applied to batch processes, where fixed bed studies should be better explored. From this review, it can be concluded that adsorption is a promising technique for OFL removal. However, it is extremely necessary to break the laboratory scale barrier and analyze possible conditions for applying these materials in treating real effluents together with combining technologies.

1. Introduction

Due to the population's increase in population and life expectancy, the consumption of pharmaceutical drugs has increased worldwide. Another factor that can aggravate the use of these substances is the emergence of new pandemics, such as COVID-19 [1]. Within this group of drugs are antibiotics. Data from 2015 confirm that 34.8 billion daily doses of antibiotics were used; based on these numbers, it is estimated that by 2030 around 84 billion will be consumed daily [2]. The consumption of antibiotics goes beyond human use; in the livestock sector alone, in 2010, around 63.151 tons were consumed, and by 2030 an increase of 67% is estimated [3]. In medicine, antibiotics are consumed to prevent or combat the growth of undesirable microorganisms [4]. Common types of antibiotics are tetracyclines (tetracycline, oxytetracycline, and doxycycline) [5], sulfonamides (sulfamethoxazole, sulfamonometoxin, sulfadimethoxine, and sulfamethazine) [6], macrolides (erythromycin, azithromycin, and clarithromycin) [7], β-lactams (ampicillin and amoxicillin) [8] and quinolones (norfloxacin, ofloxacin, ciprofloxacin, and enrofloxacin) [9]. Fluoroquinolones are the most used in treating severe bacterial infections due to their high efficacy [10]. Within this group, ofloxacin hydrochloride (OFL), whose properties are described in Table 1, is the second most used drug [11].

Table 1. Main chemical properties of OFL. Information collected from *PubChem®* database.

Molecular formula	$C_{18}H_{20}FN_3O_4$
Molecular weight	361.37 g mol^{-1}
Structure	
IUPAC name	7-fluoro-2-methyl-6-(4-methylpiperazin-1-yl)-10-oxo-4-oxa-1-azatricyclo[7.3.1.0^{5,13}]trideca-5(13),6,8,11-tetraene-11-carboxylic acid
CAS identifier	82419-36-1
Melting point	250 to 257 °C
Solubility (water)	28.3 mg mL^{-1}
log K_{ow}	-0.39
pKa$_1$ and pKa$_2$	6 and 8.5

63   The high human and animal consumption of OFL, added to the fact that the body

64   absorbs less than 10%, and the other 90% is released in the urine and feces, have made OFL

65   an emerging pollutant of great environmental importance [12–16]. Significant amounts of OFL

66   are released into water globally in their original chemical form or as metabolites [17,18]. As a

67   result, OFL has been detected in wastewater (at concentrations ranging from 100 ng L^{-1}-10 μg

68   L^{-1}), groundwater, and drinking water [19–22]. The highest levels have been observed in

69   hospitals and pharmaceutical industries effluents, with concentrations reaching up to 500 mg

70   L^{-1} [23]. Upon entering the water system, OFL can be easily absorbed and bioaccumulated by

71   plants and animals [24]. This undesirable exposure has direct effects on living organisms, flora,

72   and fauna [25], where, among the problems, the spread of bacterial resistance [26] triggers

73   an alert in the scientific community [17,27]. Due to exposure, whether by airways, dermal or

74   oral contact [28,29], it is estimated that by 2050 about 1.000.000 deaths worldwide will be

75   caused by bacterial resistance [30]. Therefore, developing and improving OFL remediation

76   technologies for the environment is essential and urgent.

77   Currently, laboratory-scale studies are being carried out to remove and degrade OFL

78   from water. The available technologies include Fenton oxidation [31], photocatalytic

79   degradation [22,32,33], sludge ozone reduction [34], anaerobic treatment [35], coagulation

80   [36], membrane treatment [37], and adsorption [38]. Each technology has positives and

81   negatives. In adsorption methodology, the adsorbate adheres to the adsorbent surface

82   employing forces mostly of a physical nature [39–41]. The efficiency of the process depends

83   on several factors, such as textural properties of the adsorbent, pH of the solution, adsorbent

84   dosage, temperature, and presence of other adsorbates in the medium in which they compete

85   for adsorptive sites, among other parameters [42,43]. Among the advantages of adsorption,

86   the simple operational design, the possibility of desorption, and the reuse of the adsorbent

87   have made this technique an object of constant study by the scientific community [44,45].

88   In the field of OFL adsorption, several adsorbents have been developed and studied.

89   Approximately 27 studies published in relevant journals were found, which presented

90   accurate results and analyses. The maximum adsorption capacity of OFL ranges from 0.3986

91   mg g^{-1} using Fe/Cu oxides composite [46] to 3702 mg g^{-1} with biochar from rice rusk as

92   adsorbents [47]. Most of the research confirmed that the adsorption of the antibiotic is

93   facilitated in conditions of pH close to neutrality between pH 7 and 8 [48–52]. Temperature

94   also greatly influenced the adsorption of OFL, where in most studies, its increase positively

95   favored the adsorption of the antibiotic from the aqueous medium [46,49,53–56]. Among the

96   other parameters, the desorption and reuse of the adsorbent [52,57–61] and the influence of

97   the coexistence of other drugs and ions in the adsorption process were also extensively

98   explored by the authors [21,38,48,49,53,57,58,62–65].

99   Still, despite the advancements in several environmental remediation technologies for

100 the adsorption of antibiotics, studies indicate a lack of selectivity for OFL removal.

101 Additionally, there is an incomplete understanding of OFL decontamination through complex

102 efficiency indicators, such as ecotoxicological assessments. This review aims to address these

103 existing gaps and promote breakthroughs in the adsorption field, including applying these

104 adsorbents on an industrial and environmental scale. This point is urgent due to the high

105 environmental demand influenced by the ecotoxicological effects of this drug, as highlighted

106 in this review. Furthermore, the inefficiency of conventional treatments at treatment stations,

107 coupled with a large part of the drug's elimination through urine, has resulted in OFL being

108 detected in various parts of the world, as extensively reported in this study. After establishing

109 these topics, this review discusses operational issues revolving around the main problems

110 encountered during OFL adsorption, such as pH, adsorbent dosage, and data interpretation.

111 Finally, this review analyzes prospects and other technologies used for OFL removal.

112 **2. Ofloxacin in the environment**

113 Antibiotics from the fluoroquinolone group are classified as emerging contaminants

114 because they are difficult to biodegrade, have high solubility and mobility in water, and most

115 of them are not absorbed by the human body and are released in the urine [66]. Another point

116 is that effluent treatment stations, mainly industrial and hospitals with a higher concentration

117 of drugs, cannot remove 100% of these compounds being released directly into water

118 resources [67], so they are frequently detected in the environment in different regions around

119 the world. For example, OFL was detected up to 160 µg L^{-1} in the industrial area of Patancheru

120 near Hyderabad in India [68]. Due to this, an alarming risk quotient of up to 6000 has been

121 reported [69]. Due to its low degradation, OFL maintains its natural biological resilience when

122 it enters the environment [70]. Therefore, when sewage effluents containing a high discharge

123 of antibiotics enter the various environmental compartments (lakes, rivers, and

124 environmental runoff), a large percentage percolates and leaches intact into groundwater, as

125 shown in Figure 1. In the OFL used in treating bacterial infections [71], only 10% is absorbed

126 by the body; the rest is released through urine and feces. This behavior is also observed in

127 animals, where livestock extensively uses these drugs. In this case, metabolic forms can occur

128 after 48 hours, where 10% is metabolized in the living organism, playing a bactericidal role in

129 treating inflammation [72].

130 **<Fig.1>**

131 Table 2 confirms that OFL has already been detected in different water compartments

132 worldwide. Studies prove the presence of OFL in surface waters of countries such as China,

133 Korea, Taiwan, Portugal, India, Vietnam, North America, and Asia, ranging from 10 to 3170 ng

134 L^{-1}. In China, OFL is a serious emerging pollutant due to the high discharges of daily

135 concentrations that enter the treatment plants and the environment, reaching 780 ± 130 ng

136 L^{-1} and 74 ± 15 ng L^{-1}, respectively [67,73]. In India, OFL was detected in surface waters in the

137 10-100 ng L-1 [74]. In Portugal, the average concentration was 120 ng L^{-1} [75], from 5 to 580

138 ng L^{-1} in Europe [20,76], 100-566 ng L^{-1} in the USA [77], and 212 to 160.000 ng L^{-1} in Indian

139 cities [78]. In effluents from industries and hospitals, the concentrations are much higher; for

140 example, in Korea where OFL was detected at around 31 mg L^{-1} [69], and in France, an average

141 daily amount of 3.7 g was observed at 0.09 g both in hospital effluents [79]. In USA effluents,

142 the concentration was 10 ng L^{-1} [80]. Due to its chemical characteristics, OFL was detected in

143 groundwater in China, ranging in concentration from 0.3 to 1199.7 ng L^{-1} [81], and in soil

144 samples in Brazil (22.2 ng L^{-1}) [82] and China (3.07-653 ng g^{-1}) [83]. Finally, countries such as

145 China [84,85], the USA [26], Sri Lanka [86], Italy [87], and France [79] report daily OFL

146 discharges at sewage treatment plants. Therefore, the environmental contamination caused

147 by OFL and the need to apply and develop technologies to mitigate this emerging contaminant

148 are evident.

149

150

151

152   Table 2. Detection of OFL in different water resources around the world.

Location	Sample matrice	Concentration (ng L^{-1})	Reference
China	effluent from the sewage treatment plant	780 ± 132	[67]
China	surface Waters	74 ± 15	[73]
China	subterranean Waters	0.3-1199.7	[81]
China (Bohai bay)	surface Waters	5100	[88]
Korea	hospital wastewater	31	[89]
Korea	surface Waters	3170	[70]
Taiwan	surface Waters	13.633	[90]
Brazil	soil samples	22.2	[82]
China	soil samples	3.07-653	[83]
Portugal	surface Waters	120	[75]
USA	wastewater effluent	10	[80]
India	surface Waters	10-100	[74]
Europe	residual Waters	5-580	[20,76]
USA	residual Waters	100-566	[77]
India	residual Waters	212-160.000	[78]
Vietnam	surface Waters	45-2867	[91]
North America	surface Waters	470-1000	[92]
Asia	surface Waters	54.8-1274	[93]
France	hospital wastewater	560-680	[79]
Italy	hospital wastewater	110-470	[87]
Sri Lanka	effluent from a sewage treatment plant	497-2.900	[86]

153   **3. Ofloxacin Ecotoxicology**

154   When OFL enters the environment, it affects aquatic biota, plants, animals, and

155   humans (Figure 2). Once in an organism, bioaccumulation and biomagnification occur [94,95].

156   Antibiotics can also alter the microbial community in water, soil, and even living organisms

157   such as plant roots, leading to new strains with antibiotic-resistance genes [96]. The new

158   strains are formed, which have antibiotic-resistance genes, leading to resistance to these

159   drugs in bacteria [97]. From this point on, infections cannot be treated with antibiotics already

160   on the market. Studies have already proven the abundance of these strains resistant to

161   sulfonamides and tetracyclines, both present in large environmental concentrations [98]. In

162   the Liaohe River basin in China, the presence of OFL promoted the dissemination of resistance

163   genes [99]. In aquatic organisms, the toxicity of OFL was analyzed with the green algae species
164   *Raphidocelis subcapitata* and the cyanobacterium *Synechococcus elongatus*; both organisms
165   were highly sensitive to the antibiotic with impairment of development and biological
166   functioning [74]. Prolonged exposure in the Daphnia magna crustacean species caused
167   offspring deterioration and infertility [100]. OFL also showed high toxicity to the freshwater
168   cladoceran *Simocephalus vetulus,* where a significant increase in forelimb rate was observed
169   [101].

170   In plants, the presence of resistance genes in the rhizosphere generated hormetic
171   effects on the growth, physiology, and development of the microbial community of the
172   species *Cyperus involucratus*. The highest accumulation of these genes was observed in the
173   roots, followed by the stem and leaves. With this, it was observed that the transport of
174   nutrients from the roots was compromised, affecting the development of the plant [102]. In
175   *Spirodela polyrhiza*, contact with OFL reduced leaf biomass, decreased reticular system
176   growth, and the phytopigment content responsible for photosynthesis [103]. In animals, OFL
177   is toxic in mammalian cells, inducing oxidative stress, lipid peroxidation, and oxidative DNA
178   damage [104]. Finally, the antibiotic has the potential for chondrotoxicity in juvenile animals,
179   such as rats [105], dogs [106], rabbits [107], non-human primates [105], and others [108].
180   Symptoms present with lameness, ulcerative erosion or cavitation of the articular cartilage of
181   weight-bearing joints, loss of chondrocytes and matrix degeneration, and blister formation
182   [105].

183   Damage in humans can be physical such as rupture of the Achilles tendon [109],
184   glaucoma [110], allergic diseases [111], retinal detachment [110], increased risk of obesity
185   [112], neurological damage, and mental disorders [113,114]. Furthermore, in women,
186   continued exposure can lead to infertility [115]. In the study by Zhang et al. [116], 102 adults
187   were in constant contact with low doses of antibiotics, including OFL, where a change in the
188   level of mitochondrial DNA methylation was observed, confirming an epigenetic modification.
189   Finally, the study by Sheng et al. [117] confirmed that OFL generates Nox2-mediated
190   intracellular reactive oxygen production by disrupting β1 integrin function and then activating
191   the EGFR-Vav2-Rac1 pathway, resulting in apoptosis. Therefore, the damage is serious and
192   should be intensified in the coming years due to the demand and consumption of antibiotics.

193 **<Fig.2>**

194 **4. Mitigation of OFL from the environment by adsorption technology**

195   When the molecule in the liquid fluid is linked to the surface of the solid, adsorption

196 occurs [118]. This link can be physical or chemical. However, most processes occur through

197 physical forces where desorption is facilitated [119]. In order to describe when the adsorbent

198 surface reaches equilibrium, equations were elaborated. The most used in studies are the

199 Langmuir[120] and Freundlich [121] equations; both are classified as isotherms, where their

200 parameters are temperature dependent [122]. In the literature, it is possible to observe the

201 successful application of these models to represent different adsorbents in removing

202 pharmaceutical compounds [123–125].

203   In addition, different sectors of society generate various types of waste daily. One

204 advantage of adsorption is that it enables the conversion of these biomasses into adsorbent

205 materials for subsequent removal of OFL from aqueous media [126]. Over the past 20 years,

206 the methods employed for producing and designing the desired morphological properties for

207 adsorbents have been improved and perfected. The current challenge is optimizing several

208 factors that can change the process result and the overall efficiency, such as pH, adsorbent

209 dosage, contact time, and OFL initial concentration. In this section, the results reported in the

210 literature for several adsorption variables are thoroughly analyzed, discussed, and displayed

211 in Table 3.

212 *4.1. Effects resulting from pH variation*

213   The pH value present in the medium in which OFL adsorption occurs greatly influences

214 the process due to factors such as the degree of ionization of the adsorbate, the charges

215 present on the surface, and the functional groups of the adsorbent [127]. Table 3 provides

216 different adsorbents' most favorable pH conditions for OFL adsorption. First, most studies

217 concerning the adsorption capacity were favored in basic conditions between pH 6.5 and 8. In

218 these cases, it was observed that the adsorption increases with the increase of the pH reaching

219 the maximum capacity and then decreases. This behavior is related to the increase in the

220 electrostatic forces of attraction between the adsorbent surface and the OFL molecules. This

221 attraction normally occurs due to the difference in charges present in the two

222   (OFL/adsorbent), which is greatly influenced by the adsorbent's zero charge point value

223   (pHPZC). With the pH below $pH_{PZC,}$ the surface is positively charged, favoring the adsorption

224   of negatively charged species. Conversely, when it is above the pH_{PZC} value, the adsorption of

225   positively charged species is favored.

226   It should be noted that the OFL pK_{a1} and pK_{a2} dissociation constants are 5.77 and 8.44

227   [49]. In this case, when the pH is below 6, the piperazine amino group is protonated, and the

228   H^+ ions in high concentrations compete with the positively charged OFL molecules, disfavoring

229   the adsorption. Between pH 6 and 9, where most studies have observed favoring OFL

230   adsorption, the existence of the zwitterionic form occurs. The protonated piperine and the

231   deprotonated carboxyl group also lead to electrostatic interactions with the positively charged

232   surface, favoring the adsorption [49,53]. Finally, the decrease in adsorption above pH 9 is due

233   to the predominance of OH^- ions corresponding to the anionic form of OFL [38].

234   In addition to the conclusions that can be observed individually regarding the analysis

235   of the morphological characterizations of each adsorbent and the implicit relations of the pK_a

236   and pH values, more information about the effect of pH can be explored based on the

237   adsorbent pH_{PZC}. The pH_{PZC} describes the pH value at which the sum of positive charges equals

238   the sum of negative charges. Thus, when electrostatic forces govern the adsorption process,

239   no adsorption should occur at the pH_{PZC} value [128]. For example, Akhtar et al. [37] found an

240   unexpected favoring of OFL adsorption when the pH was equal to 4 for the three biochars

241   produced in the study. Even predicting that electrostatic repulsion would most likely occur

242   due to the pH_{PZC} values of the adsorbents, a removal of 82.6% was observed at pH 4. The

243   justification is that cationic exchange may have occurred between the functional groups

244   containing oxygen in the coals, with the predominance of OFL in the cationic form [64]. In the

245   study by Yang et al. [64], the zeta potential of the thermal kaolin adsorbent added to the pH_{PZC}

246   favored adsorption at pH 5. As the pH_{PZC} value was 3.28 and the zeta potential was negative,

247   the adsorbent surface remained with negative charges during the augmentation in the pH of

248   the solution. At pH=5, the OFL is in its cationic form, favorable for adsorption. When the pH is

249   less than 4, more H^+ ions in the solution compete for adsorption sites. Finally, at pH above 6,

250   the OFL ions are close to being zwitterionic, converting to the anionic state with repulsion with

251   the negatively charged surface of the adsorbent.

252 **Table 3**. Parameters and maximum adsorption capacities of adsorbents for removing the OFL.

Adsorbent	pH	pH_{pzc}	Dose (g L^{-1})	T (K)	C_0 (mg L^{-1})	Isotherm Model	R^2	Nature	q_{max} (mg g^{-1})	S_{BET} (m^2 g^{-1})	Dp (nm)	Vp (cm^3 g^{-1})	Reference
Ilmenite-biochar composite	8	x	1	308	2-25	Langmuir /not linear	0.99	end	15.068	474	1.86	0.220	[48]
Oryza sativa husk ash	8	8.6	10	318	10-100	Langmuir /not linear	0.997	endo	8.16	124	6.02	0.17	[49]
N-doped activated carbon	8	8	0.2	313	110-250	Langmuir /not linear	0.9823	endo	780	1818.2	x	1.12	[53]
Biochar from rice husk	4	6.74	1	x	5-100	Langmuir /not linear	0.968	x	3702	0.144	0.0004	11.06	[47]
Biochar from sawdust	4	6.45	1	x	5-100	Langmuir /not linear	0.974	x	234.3	7.544	0.02	10.61	[47]
Biochar from municipal organic waste	4	8.49	1	x	5-100	Langmuir /not linear	0.937	x	669.5	1.99	0.0013	2.152	[47]
ZIF-8 (metal-organic frameworks)	9	x	0.71	308	5-100	Langmuir /not linear	0.99	endo	182.46	650.8	107	x	[54]
Thermal kaolin	5	3.18	0.75	298	1-15	Langmuir /not linear	0.948	x	45.27	44	21.1	0.233	[64]
Bentonite clay	8	2.7	1.2	328	0.003163-1.2654	Dubinin Radushkevick /not linear	0.954	endo	160.81	87.285	x	42.27	[56]

Material													
Rice husk	6.5	x	2	318	10-50	Langmuir /not linear	0.99	endo	35.76	23.2	1.44	0.030	[129]
Boron nitride nanosheets	8	x	0.4	298	20-160	Langmuir /not linear	0.978	x	72.5	1801.9	x	x	[130]
Hydroxyapatite/acti vated carbon (HAP/AC)	7	6-6.8	0.5	323	10-30	Langmuir /not linear	0.8731	endo	39.67	920.51	x	x	[50]
Rice husk ash	8	8.4	10	298	10-100	Langmuir /not linear	0.999	x	7.34	127.48	x	0.3696	[131]
Chitosan/Biochar Composite	6.5	6.6	0.5	298	2-20	Langmuir /not linear	0.977	x	6.64	141	x	x	[132]
AC derived from luffa sponge	6	x	0.5	293	5-30	Langmuir /not linear	0.99	exo	132	834.008	5.35	x	[11]
Magnetic carboxylated cellulose nanocrystals (M-CCNs)	7	x	2	298	50-900	Langmuir /not linear	0.99	x	58.48	x	x	x	[133]
Carboxymethyl cross-linked lignin	8	3.94	1.6667	298	18.06-90.34	Langmuir /not linear	0.994	x	458.57	x	x	x	[134]
AC from Cassava Stem	8	9.2	0.5	328	100-400	x	x	endo	58.82	847.725	1.99	0.3812	[55]
Fe/Cu oxides composite	8	4.02	0.25	313	0.01993-0.3467	Redlich-Peterson /not linear	0.99	endo	0.3986	27.8	3.41	0.093	[46]

Material													
Fe/Co bimetallic modified biochar	7	6.76	0.1	298	x	Langmuir /not linear	x	x	142.1914	496.423	4.012	0.498	[58]
Copper-Doped ZIF-8	8.5	x	1	303	120-500	Langmuir /not linear	0.98	x	599.96	1438.27	1.6124	0.7353	[21]
Fe_3O_4@MIL-100(Fe)	7	x	0.5	298	10-293	Langmuir /not linear	0.97	x	123	3546	x	x	[51]
Zeolitic Imidazolate Framework-8 (ZIF-8)	7	x	5	298	5-100	Freundlich /linear	0.99	endo	175	x	x	x	[52]
Bagasse biochar	7	x	1	313	5-20	Freundlich /linear	0.99	x	2.78	24.6043	95.56	0.05878	[59]
rGO@CuO/6A5N2TU colloidal heterostructures	8	x	1	298	5-100	Langmuir /not linear	0.97	exo	66	x	x	x	[60]
Coal fly ash	7	x	20	318	40-160	Langmuir /not linear	0.99	endo	2.643	17.5	x	x	[135]
Industrial sludge (AC)	7	7.2	5	298	5-300	Langmuir /not linear	0.965	x	21.6	4.1	x	x	[61]

253 Where x stands for not given, endo stands for endothermic, and exo stands for exothermic.

254   *4.2. Adsorbent dosage effect*

255   Of the 27 studies listed (Table 3), not all bring experiments analyzing the ideal dosage;

256   in this case, it is only informed. In OFL adsorption studies, the dosage ranged from 0.1 to 20 g

257   L^{-1}. The studies that preliminarily analyzed the dosage obtained two y-axis graphs, one to

258   represent the efficiency in the dosage of adsorbent used and the other for the achieved

259   adsorption capacity, where the point of intersection of the curves determines the optimal

260   dosage to be used in subsequent experiments [136]. Notably, higher dosages do not

261   necessarily result in greater efficiency in many cases, as the adsorbents may agglomerate and

262   lead to steric hindrance of the active sites. However, this highly depends on the nature of the

263   adsorbent and its morphological properties. It is also known that increasing the adsorbent

264   dosage favors the adsorption capacity in most adsorption processes. This effect is attributed

265   to the increased availability of sites on the surface for adsorbate molecules.[137,138].

266   Therefore, the studies confirmed that increasing the dosage led to an increase in OFL removal.

267   However, the adsorption capacity decreased. Another point that must be taken into account

268   is the economic viability, sometimes, the adsorbent dosage is doubled, and the removal

269   efficiency does not increase in the same proportion.

270   *4.3. Contact time and best-fit kinetic model*

271   Determining an effective contact time is as important as determining the q_{max} value of

272   an adsorbent, as it will directly weigh on its possible application in a scale-up process. The

273   correct projection of the kinetic time of a certain adsorbent leads to operational cost savings.

274   Unfortunately, one of the reasons why adsorption is still not widely used is that adsorption

275   saturation (which represents the point at which adsorbate molecules occupy all available

276   places on the adsorbent surface) takes a long time to be reached, mainly for most of the

277   adsorbents presented in the scientific literature. When comparing the necessary contact time

278   of other pollutants, OFL presents a moderate time; however, the variation is well diversified,

279   as shown in Table 4. The equilibrium interval varies from 20 to 1200 min. However, most

280   adsorbents present kinetics below 250 min. Adsorbents with fast rates were also observed

281   where the system reached equilibrium before 30 min of operation using chitosan/Biochar

282   Composite [132], magnetic carboxylated cellulose nanocrystals (M-CCNs) [133], Fe/Cu oxides

283   composite [46], and Fe3O4@MIL-100(Fe) [51]. The biochars from rice husk, sawdust, and

284 organic waste [47] have longer kinetics: 900, 1200, and 1200 min, respectively. These
285 differences can be explained due to differences between materials, such as surface area,
286 volume, and pore diameter. Generally, surface area and other textural parameters impact
287 adsorption capacity, but in the case of OFL, which is a large molecule, it will also impact the
288 required contact time due to the time required to overcome steric hindrance and for adequate
289 accommodation of the molecule at receptor sites.

290   In general, these studies show kinetic curves with faster adsorption rates in the first
291 minutes, where the speed decreases with time until reaching the saturation of the adsorbent.
292 This occurs because all adsorptive sites are free to accommodate OFL molecules in the first
293 few minutes. As time passes, these sites fill up; the rate slows down as the OFL molecules have
294 fewer sites to accommodate. In terms of economics and the possibility of applying the
295 adsorbent on a full scale, adsorbents with faster kinetics are preferable since the process is
296 optimized, resulting in economic benefits. However, it is always important to consider that
297 industrial-scale processes present a huge volume of effluent to be treated. Therefore,
298 developing an adsorbent with a high affinity for the pollutant is always a subject of study. The
299 speed that describes these processes and their general mechanisms is studied in adsorption
300 kinetics, following a previously established equation called the kinetic model. The most
301 popular kinetic models for adsorption are pseudo-first and pseudo-second order, followed by
302 Avrami, Elovich, Reichemberg, and Vermeulen, and the double constant- rate. The data are
303 fitted to the models, and to determine the kinetic model that best fits, the statistical
304 coefficients are calculated for the correlation coefficient (R^2), adjusted correlation coefficient
305 (R^2_{adj}), mean residual error (ARE), mean squared residual error (MSR) need to be taken into
306 account, and Bayesian information criterion (BIC) [139].

307   Specifically, for OFL adsorption, the pseudo-second-order model was predominantly
308 the one that best fitted the data, presenting the best statistical adjustments (Table 4). In this
309 case, the model presented the highest correlation coefficient (R^2) values ranging from 0.92 to
310 0.99 and the lowest values of ARE. Still, although kinetics can provide information about the
311 mechanism of accommodation of the molecule at the receptor sites, no information can be
312 obtained by these means about the forces of interaction, the energy of the sites, or the
313 position of the OFL molecule. However, when analyzing the studies by Akhtar et al. [47],

314   Antonelli et al. [56], and Bangari and Sinha. [130], and Thakur et al. [38], the authors state that

315   possibly the process was chemical in nature, with the occurrence of bonds between the OFL

316   and the surface of the adsorbents precisely due to the kinetic adjustment. In the case of the

317   study by Antonelli et al. [56] and Akhtar et al. [47], the authors did not obtain the

318   thermodynamic parameters. However, they performed desorption tests, where it can be

319   successfully observed, which could not occur if forces of a chemical nature governed the

320   adsorption. Bangari and Sinha. [130], and Thakur et al. [38] did not estimate the

321   thermodynamic parameters. Finally, in the case of the study by Yang et al. [64], the authors

322   claim when proposing an adsorption mechanism that chemisorption and physisorption

323   occurred as described in Table 5. They claim that the atoms are covalently and ionically

324   bonded with the OFL. However, the study does not present the estimate of the

325   thermodynamic parameters to validate the proposed adsorption mechanism. From these

326   observations, it can be concluded that: I) although kinetic modeling is very important, it should

327   not be the only determination made; and II) the combination of various models and estimates

328   can provide a complete view of the process.

329   **Table 4.** Contact time and kinetic model of best fit of the adsorbents used in OFL removal.

Adsorbent	Contact time (min)	Kinetic model	R^2	Reference
Ilmenite-biochar composite	180	pseudo-second order/not linear	0.99	[48]
Oryza sativa husk ash	120	pseudo-second order/not linear	0.98	[49]
N-doped activated carbon	144	general-order/not linear	0.99	[53]
Biochar from rice husk	900	pseudo-second order/not linear	0.98	[47]
Biochar from sawdust	1200	pseudo-second order/not linear	0.98	[47]
Biochar from municipal organic waste	1200	pseudo-second order/not linear	0.92	[47]
ZIF-8 (metal-organic frameworks)	x	pseudo-second order/not linear	0.99	[54]
Thermal kaolin	250	pseudo-second order/not linear	0.97	[64]
Bentonite clay	200	pseudo-second order/not linear	0.99	[56]

Rice husk	480	pseudo-second order/not linear	0.99	[129]
Boron nitride nanosheets	100	pseudo-second order/not linear	0.99	[130]
Hydroxyapatite/activated carbon (HAP/AC)	60	pseudo-second order/not linear	0.97	[50]
Rice husk ash	180	pseudo-second order/not linear	0.97	[38]
Chitosan/Biochar Composite	30	pseudo-second order/not linear	0.95	[132]
AC derived from luffa sponge	240	pseudo-second order/not linear	0.99	[11]
Magnetic carboxylated cellulose nanocrystals (M-CCNs)	20	pseudo-second order/not linear	0.99	[133]
rGO-MoS$_2$ heterostructure	240	pseudo-second order/linear	0.91	[57]
AC from Cassava Stem	120	pseudo-second order/linear	0.98	[55]
Fe/Cu oxides composite	20	Double-constant rate equation/not linear	0.99	[46]
Fe/Co bimetallic modified biochar	360	pseudo-second order/not linear	0.97	[58]
Copper-Doped ZIF-8	180	pseudo-second order/not linear	0.99	[21]
Fe$_3$O$_4$@MIL-100(Fe)	30	pseudo-second order/not linear	0.97	[51]
Zeolitic Imidazolate Framework-8 (ZIF-8)	120	pseudo-second order/not linear	0.99	[52]
Bagasse biochar	90	pseudo-second order/linear	0.99	[59]
rGO@CuO/6A5N2TU colloidal heterostructures	50	pseudo-second order/not linear	0.99	[60]
Coal fly ash	150	pseudo-second order/not linear	0.99	[135]
Industrial sludge (AC)	240	pseudo-second order/not linear	0.94	[61]

330   *4.4. Effect of temperature, best-fit isothermal model, and estimation of thermodynamic*

331   *parameters*

332   In order to carry out the correct analysis of the effect that the temperature exerts on

333   the adsorption, the interpretations provided by modeling the experimental data must be

334   discussed together. Studying the effect that the increase in temperature generates in the

335   process is fundamental in adsorption since the parameter influences the availability of

336   adsorptive sites present in the adsorbent and the mobility of adsorbate molecules. Isothermal

337   models allow the analysis of different variables under the same temperature so that the

338   mechanisms behind the interaction can be better explored, clarifying whether adsorption

339   occurs in mono or multilayers, for example [140]. These understandings can be especially

340   useful for industrial purposes, often carried out under constant conditions. Knowing how

341   different temperatures will affect the yields obtained in the process allows corrections and

342   compensatory measures to be taken as quickly as possible, avoiding large losses [141]. Added

343   to this, the use of isothermal models applied today allows the estimation of the maximum

344   capacity values of the adsorbent (q_{max}), supporting the estimation of the necessary dosage

345   values to obtain a satisfactory removal. In terms of operating costs, it is favorable that the

346   optimal performance of the adsorbent is achieved at room temperature (298 K), as this would

347   lead to lower energy consumption. Obtaining the isothermal data makes it possible to

348   estimate the thermodynamic parameters of adsorption. In this aspect, the changes in enthalpy

349   value ($\Delta H°$), the entropy variation ($\Delta S°$), and the Gibbs free energy variations ($\Delta G°$) are found.

350   Estimating these parameters is extremely important as it elucidates information about the

351   nature of the adsorption process (endothermic/exothermic). In addition to providing

352   information about the nature of the interactions (physical/chemical) involving the adsorbent

353   and the adsorbate.

354   Table 5 provides the most relevant information regarding the isotherms, such as the

355   maximum adsorption capacity and the temperature at which this performance was obtained.

356   Regarding the thermodynamic parameters, Table 5 provides the nature of the process and the

357   value of the $\Delta H°$ parameter to better understand the mechanisms that involve the adsorption

358   of OFL. First, we observed that many studies did not estimate the thermodynamic parameters,

359   making it impossible to bring new information about the interactions in the adsorption

360   process. In the studies where the temperature variation was analyzed together with the

361   thermodynamic parameters, it was possible to observe that in most cases, the increase in

362   temperature at 313, 315, and 328 K favored the adsorption of OFL ($\Delta G°>0$). This behavior

363   points to an endothermic nature ($\Delta H>0$) of the adsorbent, as observed in the following

364   adsorbents: ilmenite-biochar composite [48], *Oryza sativa* husk ash [49], N-doped activated

365   carbon [53], ZIF-8 (metal-organic frameworks) [54], bentonite clay [56], rice husk [129],

366   Hydroxyapatite /activated carbon (HAP/AC) [50], AC from Cassava Stem [55], Fe/Cu oxides

367   composite [46], Zeolitic Imidazolate Framework-8 (ZIF-8) [52] and coal fly ash [135]. Three

368   studies observed an exothermic behavior ($\Delta H°<0$), where the augmentation in temperature in

369 the system diminished the adsorption of OFL, being desirable adsorbents to be applied in real

370 conditions. The studies used rGO@CuO/6A5N2TU colloidal heterostructures [60], rGO-MoS2

371 heterostructure [57], and AC derived from luffa sponge [11] as adsorbents for the

372 temperatures of 293 and 298 K. Therefore, the exothermic behavior is not only related to

373 heterostructures, but also carbonaceous materials of vegetal origin.

374 **Table 5.** Thermodynamic parameters for OFL uptake.

Adsorbent	T (K)	ΔG^0 (KJ mol^{-1})	ΔH^0 (kJ mol^{-1})	ΔS^0 (kJ mol^{-1}. K^{-1})	Reference
Ilmenite-biochar composite	288	-22.24			
	298	-23.86	19.565	77.22	[48]
	308	-25.15			
N-doped activated carbon	298	−31.457			
	303	−31.871	3.7408	0.1178	[53]
	308	−32.461			
	313	−33.224			
ZIF-8 (metal-organic frameworks)	293	-2.30			
	298	-2.58	7.02	3.2x10^{-5}	[54]
	303	-2.70			
	308	-2.78			
Bentonite clay	298	-12.54			
	308	-13.22	7.88	6.849x10^{-2}	[56]
	318	-13.91			
	328	-14.59			
Rice husk	288	-18.37			
	303	-19.21	27.45	0.1574	[129]
	318	-23.20			
Hydroxyapatite/activated carbon (HAP/AC)	303	-11.96			
	313	-14.04	51.016	0.2078	[50]
	323	-16.12			
AC derived from luffa sponge	298	-29.87			
	303	-29.60	-40	-0.034	[11]
	308	-29.53			
AC from Cassava Stem	298	-0.068			
	308	-0.2798	10.44	0.034	[55]
	318	-0.6278			
	328	-0.9758			
Fe/Cu oxides composite	293	-3.70	4.8	0.0298	[46]

	303	-3.99			
	313	-4.99			
	293	-1.68			
Zeolitic Imidazolate Framework-8 (ZIF-8)	298	-1.92	7.06	3.0×10^{-5}	[52]
	303	-2.06			
	308	-2.13			
rGO@CuO/6A5N2TU colloidal heterostructures	303	-96.18			
	318	-98.36	-1.2887	2.8×10^{-5}	[60]
	328	-99.81			
Coal fly ash	298	-13.65	127.4	0.4732	[135]
	308	-8.72			
	318	-6.94			

375   Showing a favored adsorption efficiency with increasing temperature is not exclusive

376   to OFL. Usually, the best performance with increasing temperature is intertwined with the

377   increase in the solubility of the adsorbate in the solution. As a result, the molecules are more

378   mobile, facilitating their accommodation on the surface of the adsorbent. Therefore, even if

379   the isothermal fit can provide much information about the process, its use does not rule out

380   the need for further investigations. Regarding ΔS, most studies showed ΔS>0, indicating high

381   adsorbate-adsorbent affinity, with a characteristic increase in the randomness of the

382   solid/solution interface [142]. Studies that present negative ΔS^0 indicate a disturbance level in

383   the solid-liquid interface during the adsorption process, decreasing the degree of freedom of

384   the system. As well as the kinetic data were fitted to models, the isothermal data were

385   analyzed by estimating the parameters through models used in adsorption studies. The best

386   fit was defined by analyzing the values of the statistical parameters (R^2, R^2_{adj}, MSE, and ARE).

387   Of the 27 studies reported (Table 3), 21 showed a better fit for the Langmuir isotherm. In this

388   case, the adsorption of OFL molecules adheres through monolayer formation. Another

389   observation is that the steric hindrance imposed by the size of the OFL molecule and the

390   possibility of a surface formed by adsorptive sites distributed more orderly and

391   homogeneously may occur.

392   Regarding the Freundlich model, 4 studies were found [11,52,59,133], where all

393   obtained adjustments above 0.99. The studies by Hu et al. [133] and Yu and Wu. [52], used

394   some composite formed by the aggregation, doping, or involvement of two or more materials,

395   corroborating the Freundlich isotherm, indicating a more heterogeneous surface [143].

396   However, this rule is not always applied since studies by Kong et al. [11] and Ye et al. [59] are

397   adsorbents from carbonaceous materials, which are expected to have a more homogeneous

398   surface compatible with the Langmuir isotherm. Finally, using a less common isothermal

399   model, such as Redlich-Peterson [144], was also described in studies by Ma et al. [46] using

400   Fe/Cu oxides composite as adsorbent and obtaining a fit of 0.99. The Redlich-Peterson model

401   is not intended to combine the Langmuir and Freundlich isotherm models in any way. Instead,

402   it suggests a three-parameter equation to correct the inaccuracies of all the other two-

403   parameter equations developed [144]. Of all models, the Redlich-Peterson and Dubinin-

404   Radushkevick (are possibly the least explored, which can be attributed to the inappropriate

405   adjustment methods used in general. The study by Antonelli et al. [56] was the only one who

406   showed that the isotherms were better adjusted by the Dubinin-Radushkevick model,

407   suggesting that the process assumes multilayer adsorption and heterogeneous adsorbent

408   surface. This model is based on the adsorption potential theory and assumed that the

409   adsorption process was related to filling the micropore volume as opposed to layer-by-layer

410   adsorption on the pore walls.

411   Finally, of the analyzed studies, only three presented linear isothermal adjustment

412   [52,57,59], with R^2 of 0.99, 0.99, and 0.98, respectively. Here, it is important to emphasize that

413   the non-linearized isotherm is always preferred, mainly due to deviations and subsequent

414   errors that may reflect badly on the thermodynamic analysis [145]. The same analysis is

415   performed for the adjustments of the kinetic models, where although most of the studies used

416   non-linear models (Table 4), three studies presented a linear adjustment [55,57,59], with R^2

417   of 0.91, 0.98, and 0.99. The great point is that the surface of the adsorbent presents a limit of

418   available adsorptive sites; as these sites are occupied, the adsorption no longer presents a

419   linear behavior, as it saturates; therefore, using linear equations indicates that the data will

420   tend to be overestimated, and may not provide reliable values of the actual adsorption

421   capacity of the material [41].

422   *4.5. Effect of increasing OFL concentration and entropy contribution*

423   In most studies meticulously described in the text and tables in the previous sections,

424   the OFL concentration range has always been in the order of mg L^{-1}. The OFL concentration

425   employed in typical adsorption experiments is much higher than expected for environmental

426   samples (ng L^{-1} to µg L^{-1}). However, precisely, this factor guarantees the reliability of the data

427 collected and modeled since the error associated with low limits of detection and
428 quantification imposed by the preparation of samples from various analytical methods for low
429 concentrations is practically nil. Still, the downside of using higher concentrations of OFL is the
430 need to consider stronger adsorbate-adsorbate interactions that may reflect on the
431 adsorption process. The concentration range used in the adsorption studies varied greatly
432 from study to study, where the minimum concentration was 0.0003163 mg L^{-1} and the
433 maximum 900 mg L^{-1}. In all studies, a similar tendency is observed in that as the concentration
434 increases, the capacity also increases until saturation gives a curve in the form of a plateau.
435 This behavior is intertwined with the enhancement in the driving force gradient, clearly higher
436 at elevated concentrations, and the variation in the textural characteristics of the adsorbents,
437 such as S$_{BET}$, pore volume, and pore diameter. In the case of the driving force gradient, it is
438 generally applied to all studies since the textural characteristics must be analyzed separately
439 for each adsorbent.

440 When analyzing the influence of entropy at temperatures as low as 100.15 K, it is
441 observed that the thermodynamic equilibrium is established where the adsorbate molecules
442 are considered simple monomers. If the adsorbate molecules had unique chemical potentials
443 (μ), the coverage rate at the adsorption sites would be the same, in which case the
444 accommodation of the adsorbate molecules would be governed only by the adsorbate-
445 adsorption site's ratio ($\mu_A = \mu_B$). In this case, the total energy would necessarily be continuous
446 along the boundary between the solid-liquid phases [146]. In the case of most current
447 adsorption studies, temperatures above 298 K are used, in which case the entropy tends to
448 be even higher. With higher entropy values, the system tends to have thermal agitation
449 effects, which can limit the adsorption efficiency since adsorbate is prevented from reaching
450 the adsorptive site. In systems where other ions or adsorbates occur, competitive adsorption
451 occurs; in these cases, the entropic effects are even more severe due to the diversification of
452 molecular sizes and energies. This subject is better discussed in item 6.

453 *4.6. Adsorption mechanisms*

454 So far, we have discussed the influences that parameters such as temperature and pH
455 can have on the efficiency of the process, as well as how much information can be obtained
456 from isothermal and kinetic modeling. Notwithstanding, not all papers give a piece of clear

understanding of the interactions at the interface of the adsorbent and OFL molecules. Some papers claimed an interaction mechanism performed equilibrium or thermodynamic studies or FTIR analyses. In addition to these, however, several other analyses can be employed to provide insights into possible interaction mechanisms. Most of these analyses consider the adsorbent rather than the adsorbate: the pH_{PZC} can be determined by acid-base titration, and the S_{BET} and pore properties can be determined by N_2 ads/desorption. Here, it is important to emphasize that the nature of the adsorbent can determine the type of interaction, but it is the understanding of the OFL molecular equilibria in the experimental conditions that will allow the process to advance or not. To confirm whether the nature of the mechanism occurs by physical or chemical forces, that is, whether the process is physisorption or chemisorption, the thermodynamic parameters must be estimated.

Approximately 17 studies proposed adsorption mechanisms based mainly on possible electrostatic interactions, as shown in Table 6. The electrostatic interactions are physical and may correspond to hydrogen bonding, Van der Walls forces, and hydrophobic and polar interactions. For aromatic compounds such as OFL, π-π, and n-π interactions have also been proposed as possible contributing effects. When analyzing the magnitude of ΔH^0 in these studies, all were below 80 kJ mol^{-1} [147], confirming the physical nature of the process. It should be noted that only under conditions of $\Delta H^0 > 200$ kJ mol^{-1} is it indicated that chemosorption occurs [148–150]. A few studies indicated that chemical bonds also occurred in addition to physical interactions, and each of these studies was analyzed separately. In the study by Yu and Wu. [54], the authors claim that based on the FTIR spectra, the -COOH group is active in chemical binding sites with the OFL molecule forming unsaturated divalent metal complexes with adsorbent. However, when analyzing the magnitude of ΔH^0, it presents a value of only 7.02 kJ mol^{-1}, which confirms that interactions of a chemical nature would not be possible to occur. The same problem is presented in the work of Yu and Wu. (2022), where despite being another adsorbent, the magnitude of ΔH^0 was also 7.02 kJ mol^{-1}. Similar observations are made in the study by Ma et al. [46], where the authors suggested that complexation occurred between the adsorbent Fe/Cu oxides composite with OFL; however, the ΔH^0 is 1.47 kJ mol^{-1}. The studies by Yang et al. [64] and Gao et al. [134] state that chemisorption occurs through the application of simulations of the density functional calculus theory (DFT); however, they do not present the estimate of thermodynamic parameters to

488   corroborate with the conclusions obtained. Finally, in the study by Hao et al. [58], the authors

489   state that there was an exchange of electrons through hydrogen, however, it cannot interact

490   as an electron donor only through hydrogen bonds. Finally, in the study of Singh and

491   Srivastava. [61], the authors also claim that there was an exchange of electrons, but they do

492   not justify the hypotheses that led to this statement.

493

494   **Table 6.** Mechanism of OFL uptake from aqueous medium ($pK_1 = 6$; $pK_2 = 8.5$).

Adsorbent	Adsorption mechanism	Reference
Ilmenite-biochar composite	hydrogen bonding formation and π-π interactions	[48]
N-doped activated carbon	van der Waals forces, hydrogen bonds, and electrostatically attracting	[53]
Biochar from rice husk	hydrogen bonds and polar interactions	[47]
Biochar from sawdust	hydrogen bonds and polar interactions	[47]
Biochar from municipal organic waste	hydrogen bonds and polar interactions	[47]
ZIF-8 (metal-organic frameworks)	strong hydrogen bonding, complexation of unsaturated metals, and π–π stacking	[54]
Thermal kaolin	chemosorption and electrostatic interactions	[64]
Rice husk	electrostatic interaction	[129]
Hydroxyapatite/activated carbon (HAP/AC)	strong hydrogen bonding	[50]
Carboxymethyl cross-linked lignin	hydrogen bonding, electrostatic attraction, electron-donor-π-π-acceptor interactions, and negative charge-assisted hydrogen bonding	[134]
AC from Cassava Stem	physisorption	[55]
Fe/Cu oxides composite	hydrogen bonds, π-π stacking interactions, surface complexation, hydrophobic interaction	[46]
Fe/Co bimetallic modified biochar	electrostatic interactions, hydrogen bonding, hydrophobic interactions, complexation, and π–π electron donor-acceptor interactions	[58]
Copper-Doped ZIF-8	π-π interaction	[21]
Fe₃O₄@MIL-100(Fe)	π-π interaction and H-bonding	[51]
Zeolitic Imidazolate Framework-8 (ZIF-8)	complexation of unsaturated metals, hydrogen bonding, and electrostatic interactions	[52]
Bagasse biochar	π-π bond interactions, hydrophobic interactions, hydrogen bonds, electrostatic interactions, and ion exchange	[59]
rGO@CuO/6A5N2TU colloidal heterostructures	Coordinate bond, π–π stacking, and hydrogen bonding	[60]

| Industrial sludge (AC) | electron donor-
acceptor interactions, π-π interaction,
and H-bonding | [61] |

4.7. Morphological properties and performance of adsorbents developed for OFL adsorption

496   When the adsorbent properties could influence its adsorption capacity, the S_{BET} is one of

497   the most crucial structural features of the adsorbent. Regarding OFL adsorption, it is possible

498   to observe that the parameter does not always determine whether the adsorbent has a high

499   removal efficiency. Previously, in Table 3, it is possible to observe three situations: i)

500   adsorbents with high surface areas and good adsorption capacity; ii) adsorbents with low

501   surface areas but with good adsorption capacities; iii) adsorbents with low surface areas and

502   low OFL adsorptive performance; iv) adsorbents with high surface area and low adsorption

503   capacity. In the first situation, we have the N-doped AC [53] with an S_{BET} of 1818 m^2 g^{-1}

504   obtaining a q= 780 mg g^{-1}, whereas the hydroxyapatite AC [50] with an S_{BET} of 921 m^2 g^{-1}

505   obtained a q= 39.67 mg g^{-1}, a good performance since the concentration range used was low.

506   The excellent capacity of 599 mg g^{-1} was obtained with copper-doped ZIF-8 with a high S_{BET} of

507   1438 m^2 g^{-1} [21]. In the second situation, Antonelli et al. [46] study used bentonite clay with

508   an S_{BET} of 87 m^2 g^{-1}. However, the capacity was high (160.8 mg g^{-1}). The two biochar produced

509   in the study by Akhtar et al. [47] present S_{BET} of only 0.144 and 1.99 m^2 g^{-1}, but the capacities

510   of both materials were high, being 3702 and 669.5 mg g^{-1}, respectively. In the third situation,

511   the coal fly ash material had an area of only 17.5 m^2 g^{-1}, where a low q= 2.643 mg g^{-1} was also

512   observed [135]. The same situation was observed in the study by Jaswal et al. [57], where

513   capacity (37.31 mg g^{-1}) and surface area (17.17 m^2 g^{-1}) showed low values. Finally, the fourth

514   situation is the adsorbent nitride nanosheets with a large area of 1801.9 m^2 g^{-1}, but the

515   capacity was only 72.5 mg g^{-1} [130], and the composite Fe3O4@MIL-100 (Fe) with a good

516   surface area 3546 m^2 g^{-1} but the capacity was only 123 mg g^{-1} [51].

517   This indicates that in addition to the surface area, other factors influence the adsorbent's

518   performance, such as the development of pores and their total volume, the pore size

519   distribution, the particle size of the adsorbent, and the functional moieties available in the

520   adsorbent surface. Determining the zeta potential of the adsorbent is also important because

521   it determines the existing surface charges according to the pH variation of the solution, which

522   will reflect on the strength of the interaction. Thus, all these factors need to be considered

523 before a mechanism is proposed, with special attention to the difference in adsorption kinetics

524 and mass transfer rate for porous and non-porous adsorbents, as discussed and generally

525 demonstrated by Sircar [151].

5. Regeneration and reuse

527 One of the great advantages of adsorption is the possibility of applying the same

528 adsorbent several times. Desorption is the opposite process of adsorption. Therefore it occurs

529 when the adsorbate migrates from the surface of the adsorbent to the solution (Figure 3).

530 Therefore, it must have good desorption capacity for several cycles [152]. An adsorbent that

531 maintains its removal potential little changed as desorption occurs is a competitive,

532 sustainable, and economical material for application on an industrial or environmental scale.

533 On the other hand, the low reuse indicates a high cost of the adsorbent, which is not of interest

534 in the industrial market.

535 **<Fig.3>**

536 The analysis of the potential for desorption and reuse of adsorbents was well studied

537 as it is observed that 13 studies (Table 7) presented the number of cycles that each material

538 endured maintaining a removal at viable levels to be applied again. Every time adsorbate is

539 removed from the material's surface, an eluent must be applied to remove the pollutant from

540 the surface. In the case of the listed studies, the following eluents were successfully used:

541 ethanol, acetic acid, sodium chloride, methanol, and hydrochloric acid. Eluent choice is

542 paramount; the ideal is to use a compound that is not toxic since it will generate a large volume

543 of residual effluent, which must be treated before being released into the environment. In

544 most studies, the adsorbents maintained good removal efficiency after 3 regeneration cycles

545 (> 73.9%). It was also possible to observe materials with good yield after 4 (> 70%) and 5 cycles

546 (56.1%). The magnetic carboxylated cellulose nanocrystals (M-CCNs) adsorbent [133] was the

547 most promising since, after 7 cycles, it maintained its removal above 70%, using a 30% acetic

548 acid/methanol solution as eluent. Finally, another point to be observed is that thermal

549 regeneration presents an excellent regeneration alternative since it involves energy

550 expenditure but has a lower potential for pollution since new chemical reagents are not added

551 that would be present in the final effluent.

552   **Table 7.** Summary of OFL desorption and reuse.

Adsorbent	Eluent	Number of cycles (n)	Retained after n cycles (%)	Reference
Ilmenite-biochar composite	Ethanol (C_2H_6O)	3	> 90	[48]
N-doped activated carbon	Acetic acid (CH_3COOH)	3	>74.3	[53]
ZIF-8 (metal-organic frameworks)	Sodium chloride (NaCl)	4	>77.3	[54]
Thermal kaolin	Methanol (CH_3OH)	5	>83.4	[64]
Bentonite clay	Heating at 500 °C (OFL decomposition temperature is between 250 and 257 °C)	3	>93.06	[56]
Rice husk	Heating at 200 °C	3	>73.9	[129]
Magnetic carboxylated cellulose nanocrystals (M-CCNs)	30% acetic acid/metanol (CH_3COOH/CH_3OH)	7	>70	[133]
rGO-MoS$_2$ heterostructure	x	3	>76	[57]
Fe/Co bimetallic modified biochar	Acetic Acid (CH_3COOH)	5	> 89.31	[58]
Bagasse biochar	x	5	>56.1	[59]
rGO@CuO/6A5N2TU colloidal heterostructures	Hydrochloric acid (HCl)	4	>70	[60]
Industrial sludge (AC)	Thermal regeneration	5	>59	[61]
Zeolitic Imidazolate Framework-8 (ZIF-8)	Methanol (CH_3OH)	4	>83.6	[52]

553   **6. Competitive adsorption**

554   When analyzing the potential of an adsorbent, it is always important to measure its

555   performance under real conditions. Therefore, real effluents are never unique mixtures with

556   the presence of a single molecule. Quite the contrary, real effluents contain several pollutants,

557   salts, and other compounds. Therefore, it is important to carry out competitive adsorption

558   studies, as it elucidates the affinity of the adsorbent for a specific adsorbate in light of other

559   competing species [153]. In the case of OFL adsorption, several studies analyzed this behavior,

560   as shown in Table 8. In the study by Dhiman et al. [49], when adding ciprofloxacin with OFL, it

was observed that antagonism occurred, where the effect of the mixture was smaller than the individual OFL in the mixture since the adsorption capacity of OFL decreased from 3.11 to 2.70 mg g^{-1} for the concentration of 40 mg L^{-1}. The presence of paracetamol also decreased OFL adsorption to 71%, where it was observed that as the concentration of paracetamol increased, the greater the negative effect on OFL adsorption [38]. Awasthi et al. [55] analyzed the adsorption of tetracycline and OFL antibiotics from water using a PVDF/BNNSs nanocomposite membrane as an adsorbent, where it showed good adsorption capacity. However, it was found that tetracycline exhibited preferential adsorption over OFL.

In the study by Liu et al. [48], it was observed that the removal was above 90%, where the adsorbent's performance was not impaired. The study by He et al. [53] analyzed the effect of adsorption through various ions, where it was possible to conclude that: the presence of K$^+$ and Na$^+$ did not interfere with the adsorption of OFL since the presence of Ca^{2+} and Mg^{2+} decreased the capacity to 122 mg g^{-1} and 130 mg g^{-1}, respectively. In this case, alkaline earth metal cations (Mg^{2+} and Ca^{2+}) bound more strongly to the adsorption sites, and their larger hydration radii caused strong electron repulsion [154]. SO$_4^{2-}$ and HPO$_4^{2-}$ ions increased 36 mg·g^{-1} and 32 mg g^{-1} of adsorption, respectively. This could be due to hydrolysis and the formation of a small number of hydrogen bonds. The study by Yang et al. [64] also analyzed the effect of Na$^+$, K$^+$, Mg$^{2+,}$ and Ca^{2+} ions on OFL adsorption, where it was observed that the first two had little interference with adsorption. However, Mg^{2+} and Ca^{2+} reduced adsorption by 33 and 46%, respectively. It indicated a competition of the positively charged OFL molecules with the remaining cations present in the solution. In the study by Hao et al. [58], the authors revealed that SO$_4^{2-}$, Cl$^-$, Ca$^{2+,}$ and Mg^{2+} promoted OFL adsorption, whereas NO$_3^-$, CO$_3^{2-}$ and PO$_4^{3-}$ ions significantly decreased adsorption and Na$^+$ and K$^+$ did not interfere with adsorption, authors did not provide values in terms of removal. The opposite result was observed in the study by Wang et al. [21], where Cl$^-$ and SO$_4^{2-}$ ions decreased OFL adsorption (the authors did not report values). Finally, Jaswal et al. [57] analyzed the adsorbent's performance in wastewater with a high organic matter content and various ions. Adsorbent performance was strongly affected, with removal decreased to 28%.

Table 8. Summary of OFL competitive adsorption.

Adsorbent	Competing species	Maximum change with competing species	Reference
Oryza sativa husk ash	Ciprofloxacin	< 3.11 to 2.70 mg g^{-1}	[49]
Ilmenite-biochar composite	Tap water	> 90%	[48]
Ilmenite-biochar composite	Yellow River water	> 90%	[48]
N-doped activated carbon	K$^+$, Na$^+$	not interfere	[53]
N-doped activated carbon	Ca^{2+}	< 122 mg g^{-1}	[53]
N-doped activated carbon	Mg^{2+}	< 130 mg g^{-1}	[53]
N-doped activated carbon	SO$_4^{2-}$	> 36 mg g^{-1}	[53]
N-doped activated carbon	HPO$_4^{2-}$	> 32 mg g^{-1}	[53]
Thermal kaolin	Mg^{2+}	< 33%	[64]
Thermal kaolin	Ca^{2+}	< 46%	[64]
Rice husk ash	Paracetamol	< 71 %	[38]
Fe/Co bimetallic modified biochar	SO$_4^{2-}$, Cl$^-$, Ca^{2+} and Mg^{2+}	>	[58]
Fe/Co bimetallic modified biochar	NO$_3^-$, CO$_3^{2-}$ and PO$_4^{3-}$	<	[58]
Fe/Co bimetallic modified biochar	Na$^+$ and K$^+$	not interfere	[58]
Copper-Doped ZIF-8	Cl$^-$ and SO$_4^{2-}$	<	[21]
rGO-MoS$_2$ heterostructure	Wastewater water	< 28%	[57]

7. Application of auxiliary technologies and coupled methods in OFL adsorption

Although adsorption technologies show exceptional results, several studies indicate that coupled methods can provide even better results in removing pollutants [155,156]. When analyzing the literature, the technologies applied, mostly on a laboratory scale, in removing OFL, we observed that advanced oxidation processes (photocatalysis and photo-Fenton) are preferred by most studies published after 2020. Compared with adsorption, the great advantage of these methods is that the pollutant is mineralized/degraded and does not generate secondary pollution. However, just like adsorption, the great challenge is

601   overcoming the laboratory scale barrier by applying these processes on a real scale. Most

602   studies show good efficiency in samples containing OFL [157–159], but in complex samples,

603   the photocatalytic efficiency is low. One of the main factors is the presence of suspended

604   solids that block light penetration, increasing the recombination of photogenerated charge

605   carriers. The main focus is to improve this performance through more complex samples and

606   to reduce operational costs through the application of new catalysts. It is also possible to

607   observe other forms of OFL catalytic degradation that can be found in the literature, such as

608   electrocatalysis [160], Fenton oxidation [161], catalytic oxidation [162], and ozonation [163].

609   More specifically, the Fenton and catalytic oxidation processes have shown high

610   degradation efficiency of OFL molecules. However, like all technologies, this method also has

611   disadvantages; its high cost added to the need to use by-products (bases and acids) to balance

612   the reaction (Fe^{2+}/Fe^{3+}), making this technology not 100% clean. Therefore, adsorption is still

613   a more viable process in terms of costs. However, the big issue here is not to establish the

614   "best" technology or the one that has the most advantages over the other but to seek the

615   application in a coupled manner, such as the application of ozonation followed by adsorption

616   [164]. Another alternative explored is catalytic oxidation by humid air, which also involves the

617   generation of highly oxidizing species. However, unlike simple photocatalysis, it uses high

618   temperatures. Concerning OFL, no studies were found. However, the technique presented

619   limitations for other drug compounds, where performance can be improved using mesopores

620   AC. However, studies that optimize the process to reduce operating costs are still necessary.

621   In addition to advanced oxidation processes, other developments involving classic

622   water treatment methods were carried out. As a way to enhance coagulation, for example,

623   electrocoagulation emerges as an emerging method that combines the benefits and functions

624   of conventional coagulation, flotation, adsorption, precipitation, discharge, and

625   electrochemical reactions, including cathodic reduction and anodic oxidation [165]. Among its

626   advantages, one can mention its high versatility, easy control, and high selectivity [166].

627   Unfortunately, this technique depends on many factors to be efficient, as it is very sensitive

628   to changes in several parameters [167]. In the literature, studies of electrocoagulation for

629   removing OFL are limited. However, in the study by Mokni et al. (2022), the method was

630   applied for the first time in OFL, where it was observed that the Al electrode is effective for

631 OFL removal where 72% of OFL is removed by 40 min electrolysis time, and a maximum of
632 78% is reached after 105 min.

633   Finally, new green approaches have also been shown to be possible and effective in
634 the literature, including applying plants and microorganisms to wastewater treatment
635 solutions to remove a wide variety of toxic organic pollutants, including OFL and
636 pharmaceutical compounds. The study by Maldonado et al. [168] illustrated the potential
637 application of duckweed (*Lemna* sp.) and tree fern (*Azolla* sp.) in the removal of
638 pharmaceutical residues in water, focused on a mixture of antibiotics containing OFL. The
639 study by Akerman-Sanchez et al. [169] analyzed the bioaccumulation potential of fungal
640 biomass in the bioremediation of a mixture of pharmaceutical pollutants, a method aimed at
641 bioengineering of water decontamination. Martinez-Ruiz et al. [170] performed microalgae-
642 assisted green bioremediation of leachates rich in water pollutants and recovery of source
643 products.

644 **8. Knowledge gap and future prospects**

645   Antibiotics such as ofloxacin hydrochloride are consumed in all countries of the globe.
646 However, export numbers, daily consumption, environmental presence, and concentration
647 control, mainly for industrial and hospital effluents, are still insufficient and little inspected by
648 Organs competent bodies. Therefore, it is highly necessary to improve the set of information
649 with control over the OFL production and commercialization market, leading to greater
650 accessibility of data for society and especially for the scientific community. Seeking to improve
651 OFL mitigation technologies without including a broader point of view as information on the
652 pollution caused by these drugs in industrial effluents is insufficient. Therefore, there must be
653 interest and cooperation on both sides; added to this, applying specific legislation and the
654 commitment of public bodies would be the ideal scenario. Another important issue is that the
655 major concern of industries is the final cost, and the scientific community is not always focused
656 on this issue. For example, a large part of the adsorption operating costs is the adsorbent
657 manufacture. However, studies that analyze this variable are still scarce, and even those that
658 estimate do not provide clear data from real perspectives. In order to overcome this problem,
659 hierarchical changes need to be made, ranging from the way science is produced to the
660 demand imposed by the market.

661   Now, let us look at prospects. It is to be expected that, in addition to increasing interest

662   in understanding and controlling OFL pollution, ongoing adsorption studies will incorporate

663   more sophisticated models that allow i) to predict phenomena and ii) to understand the

664   adsorption mechanisms on a microscopic scale. Over the past 10 years, machine learning and

665   deep learning have been explored for adsorption data prediction, allowing us to estimate how

666   changing certain parameters would affect the process without exploring time and money.

667   Furthermore, the development and establishment of new isothermal models that rely on a

668   statistical physics approach, incorporating the canonical grand ensemble perspective, has

669   allowed chemists and engineers to take back control and target specific synthetic points to

670   improve key structural changes in adsorbents, making them even more effective at removing

671   pollutants. Although in addition, most studies involve small-scale systems, while large-scale

672   studies include a fixed-bed column. Regarding the adsorption of OFL, the study by Antonelli

673   et al. [56] evidenced using clay as an adsorbent in a fixed bed column. It can operate for up to

674   140 hours with the removal of practically 100% of the OFL antibiotic; in the same study, the

675   authors suggest that the adsorbent is promising in studies involving even lower concentrations

676   and close to those that occur in the environment (for example, ng L^{-1} or μg L^{-1}).

677   Finally, studies using neural networks and fuzzy inference systems have not been used

678   for modeling and optimizing OFL uptake. Computer-based mechanistic modeling techniques

679   have also not been reported. In addition, the application of mass transfer models [118,171]

680   should be applied to OFL adsorption to elucidate the mechanisms involved in antibiotic

681   adsorption. These are also gaps in knowledge and can serve as a basis for future investigations

682   by other researchers.

683   **9. Conclusion**

684   Although current and future perspectives indicate the extreme urgency of improving

685   OFL mitigation technologies for the environment, not all agencies and sectors of society are

686   interested and concerned. Due to these factors, technologies such as adsorption are being

687   improved. Several adsorbents were analyzed, and most have good adsorption capacity in pH

688   conditions close to neutrality. Of the 27 articles, not all analyzed the effect temperature exerts

689   on the adsorbent's performance. However, those that analyzed the increase in this parameter

690   favored adsorption. The maximum capacities were quite varied, and it was observed that the

surface area does not always determine the efficiency of the adsorbent. For most studies, the materials show moderate kinetics where the system tended to come to equilibrium before 250 min. Thermodynamic parameters confirmed the endothermic nature of most studies, where physical interactions were predominant in the processes. The coexistence of ions in the solution can positively or negatively interfere with the adsorption, with cases where no interference was observed. Following this line, using adsorption technology in conjunction with other techniques should be an object of study, mainly to break the barrier between the scientific community and society. Taking technological advances in contaminant mitigation processes is undoubtedly a great challenge for the coming years.

References

[1]   L.R. Gonçalves, M.M. Roberto, A.P.A. Braga, G.B. Barozzi, G.S. Canizela, L. de Souza Gigeck, L.R. de Souza, M.A. Marin-Morales, Another casualty of the SARS-CoV-2 pandemic—the environmental impact, Environ. Sci. Pollut. Res. 29 (2022) 1696–1711. https://doi.org/10.1007/s11356-021-17098-x.

[2]   E.Y. Klein, T.P. Van Boeckel, E.M. Martinez, S. Pant, S. Gandra, S.A. Levin, H. Goossens, R. Laxminarayan, Global increase and geographic convergence in antibiotic consumption between 2000 and 2015, Proc. Natl. Acad. Sci. U. S. A. 115 (2018) E3463–E3470. https://doi.org/10.1073/pnas.1717295115.

[3]   T.P. Van Boeckel, C. Brower, M. Gilbert, B.T. Grenfell, S.A. Levin, T.P. Robinson, A.

Teillant, R. Laxminarayan, Global trends in antimicrobial use in food animals, Proc. Natl. Acad. Sci. U. S. A. 112 (2015) 5649–5654. https://doi.org/10.1073/pnas.1503141112.

[4] K.W. Goyne, J. Chorover, J.D. Kubicki, A.R. Zimmerman, S.L. Brantley, Sorption of the antibiotic ofloxacin to mesoporous and nonporous alumina and silica, J. Colloid Interface Sci. 283 (2005) 160–170. https://doi.org/10.1016/j.jcis.2004.08.150.

[5] C.U. Chukwudi, Harvey_Ions&FS_ScanElectronMicrosc1972II,409-419.1980.pdf, 60 (2016) 4433–4441. https://doi.org/10.1128/AAC.00594-16.Address.

[6] P. Cliquet, E. Cox, W. Haasnoot, E. Schacht, B.M. Goddeeris, Generation of group-specific antibodies against sulfonamides, J. Agric. Food Chem. 51 (2003) 5835–5842. https://doi.org/10.1021/jf034316c.

[7] G.P. Dinos, The macrolide antibiotic renaissance, Br. J. Pharmacol. 174 (2017) 2967–2983. https://doi.org/10.1111/bph.13936.

[8] L. Balsalobre, A. Blanco, T. Alarcón, Beta-lactams, Antibiot. Drug Resist. (2019) 57–72. https://doi.org/10.1002/9781119282549.ch3.

[9] H.R. Park, T.H. Kim, K.M. Bark, Physicochemical properties of quinolone antibiotics in various environments, Eur. J. Med. Chem. 37 (2002) 443–460. https://doi.org/10.1016/S0223-5234(02)01361-2.

[10] D. Zhang, Y. Wang, Functional protein-based bioinspired nanomaterials: From coupled proteins, synthetic approaches, nanostructures to applications, Int. J. Mol. Sci. 20 (2019). https://doi.org/10.3390/ijms20123054.

[11] Q. Kong, X. He, L. Shu, M. Miao, Ofloxacin adsorption by activated carbon derived from luffa sponge : Kinetic, isotherm, and Process Saf. Environ. Prot. 112 (2017) 254–264. https://doi.org/10.1016/j.psep.2017.05.011.

[12] J.R. De Andrade, M.F. Oliveira, M.G.C. Da Silva, M.G.A. Vieira, Adsorption of Pharmaceuticals from Water and Wastewater Using Nonconventional Low-Cost Materials: A Review, Ind. Eng. Chem. Res. 57 (2018) 3103–3127. https://doi.org/10.1021/acs.iecr.7b05137.

[13] M.A. Al-Omar, Chapter 6 Ofloxacin, 2008. https://doi.org/10.1016/S1871-5125(09)34006-6.

[14] C. Deng, X. Pan, D. Zhang, Influence of ofloxacin on photosystems I and II activities of Microcystis aeruginosa and the potential role of cyclic electron flow, J. Biosci. Bioeng. 119 (2015) 159–164. https://doi.org/10.1016/j.jbiosc.2014.07.014.

751   [15]   M.S. de Ilurdoz, J.J. Sadhwani, J.V. Reboso, Antibiotic removal processes from water &
752   wastewater for the protection of the aquatic environment - a review, J. Water Process
753   Eng. 45 (2022) 102474. https://doi.org/10.1016/j.jwpe.2021.102474.

754   [16]   X. Tong, X. Wang, X. He, K. Xu, F. Mao, Effects of ofloxacin on nitrogen removal and
755   microbial community structure in a constructed wetland, Sci. Total Environ. 656 (2019)
756   503–511. https://doi.org/10.1016/j.scitotenv.2018.11.358.

757   [17]   M. Feng, Z. Wang, D.D. Dionysiou, V.K. Sharma, Metal-mediated oxidation of
758   fluoroquinolone antibiotics in water: A review on kinetics, transformation products,
759   and toxicity assessment, J. Hazard. Mater. 344 (2018) 1136–1154.
760   https://doi.org/10.1016/j.jhazmat.2017.08.067.

761   [18]   X.J. Wen, C.G. Niu, L. Zhang, C. Liang, G.M. Zeng, A novel Ag2O/CeO2 heterojunction
762   photocatalysts for photocatalytic degradation of enrofloxacin: possible degradation
763   pathways, mineralization activity, and an in-depth mechanism insight, Appl. Catal. B
764   Environ. 221 (2018) 701–714. https://doi.org/10.1016/j.apcatb.2017.09.060.

765   [19]   F.F. Sodré, C.C. Montagner, M.A.F. Locatelli, W.F. Jardim, Ocorrência de Interferentes
766   Endócrinos e Produtos Farmacêuticos em Águas Superficiais da Região de Campinas
767   (SP, Brasil), J. Brazilian Soc. Ecotoxicol. 2 (2007) 187–196.
768   https://doi.org/10.5132/jbse.2007.02.012.

769   [20]   E.M. Golet, I. Xifra, H. Siegrist, A.C. Alder, W. Giger, Environmental exposure assessment
770   of fluoroquinolone antibacterial agents from sewage to soil, Environ. Sci. Technol. 37
771   (2003) 3243–3249. https://doi.org/10.1021/es0264448.

772   [21]   X. Wang, Y. Zhao, Y. Sun, D. Liu, Highly Effective Removal of Ofloxacin from Water with
773   Copper-Doped ZIF-8, Molecules. 27 (2022) 1–13.
774   https://doi.org/10.3390/molecules27134312.

775   [22]   S. Babić, M. Periša, I. Škorić, Photolytic degradation of norfloxacin, enrofloxacin, and
776   ciprofloxacin in various aqueous media, Chemosphere. 91 (2013) 1635–1642.
777   https://doi.org/10.1016/j.chemosphere.2012.12.072.

778   [23]   A. Maged, J. Iqbal, S. Kharbish, I.S. Ismael, A. Bhatnagar, Tuning tetracycline removal
779   from aqueous solution onto activated 2:1 layered clay mineral: Characterization,
780   sorption and mechanistic studies, J. Hazard. Mater. 384 (2020) 121320.
781   https://doi.org/10.1016/j.jhazmat.2019.121320.

782   [24]   T. Yamaguchi, M. Okihashi, K. Harada, Y. Konishi, K. Uchida, M.H.N. Do, H.D.T. Bui, T.D.

Nguyen, P. Do Nguyen, V. Van Chau, K.T. Van Dao, H.T.N. Nguyen, K. Kajimura, Y. Kumeda, C.T. Bui, M.Q. Vien, N.H. Le, K. Hirata, Y. Yamamoto, Antibiotic residue monitoring results for pork, chicken, and beef samples in Vietnam in 2012-2013, J. Agric. Food Chem. 63 (2015) 5141–5145. https://doi.org/10.1021/jf505254y.

[25] M.B. Ahmed, J.L. Zhou, H.H. Ngo, W. Guo, Adsorptive removal of antibiotics from water and wastewater: Progress and challenges, Sci. Total Environ. 532 (2015) 112–126. https://doi.org/10.1016/j.scitotenv.2015.05.130.

[26] N. Kemper, Veterinary antibiotics in the aquatic and terrestrial environment, Ecol. Indic. 8 (2008) 1–13. https://doi.org/10.1016/j.ecolind.2007.06.002.

[27] Z. Feng, K. Odelius, G.K. Rajarao, M. Hakkarainen, Microwave carbonized cellulose for trace pharmaceutical adsorption, Chem. Eng. J. 346 (2018) 557–566. https://doi.org/10.1016/j.cej.2018.04.014.

[28] G. Hamscher, H.T. Pawelzick, S. Sczesny, H. Nau, J. Hartung, Antibiotics in dust originating from a pig-fattening farm: A new source of health hazard for farmers? Environ. Health Perspect. 111 (2003) 1590–1594. https://doi.org/10.1289/ehp.6288.

[29] R. Paul, S. Gerling, M. Berger, K. Blümlein, U. Jäckel, S. Schuchardt, Occupational Exposure to Antibiotics in Poultry Feeding Farms, Ann. Work Expo. Heal. 63 (2019) 821–827. https://doi.org/10.1093/annweh/wxz047.

[30] A. Langdon, N. Crook, G. Dantas, The effects of antibiotics on the microbiome throughout development and alternative approaches for therapeutic modulation, Genome Med. 8 (2016). https://doi.org/10.1186/s13073-016-0294-z.

[31] X. Tian, H. Jin, Y. Nie, Z. Zhou, C. Yang, Y. Li, Y. Wang, Heterogeneous Fenton-like degradation of ofloxacin over a wide pH range of 3.6–10.0 over modified mesoporous iron oxide, Chem. Eng. J. 328 (2017) 397–405. https://doi.org/10.1016/j.cej.2017.07.049.

[32] T.J. Al-Musawi, M. Yilmaz, A.A. Ramírez-Coronel, G.R.L. Al-Awsi, E.R. Alwaily, A. Asghari, D. Balarak, Degradation of amoxicillin under a UV or visible light photocatalytic treatment process using Fe2O3/bentonite/TiO2: Performance, kinetic, degradation pathway, energy consumption, and toxicology studies, Optik (Stuttg). 272 (2023). https://doi.org/10.1016/j.ijleo.2022.170230.

[33] G.Z. Kyzas, N. Mengelizadeh, M. Khodadadi Saloot, S. Mohebi, D. Balarak, Sonochemical degradation of ciprofloxacin by hydrogen peroxide and persulfate activated by

815   ultrasound and ferrous ions, Colloids Surfaces A Physicochem. Eng. Asp. 642 (2022)

816   128627. https://doi.org/10.1016/j.colsurfa.2022.128627.

817   [34]   L. Wang, Y. Li, W. Ben, J. Hu, Z. Cui, K. Qu, Z. Qiang, In-situ sludge ozone-reduction

818   process for effective removal of fluoroquinolone antibiotics in wastewater treatment

819   plants,   Sep.   Purif.   Technol.   213   (2019)   419–425.

820   https://doi.org/10.1016/j.seppur.2018.12.062.

821   [35]   H.Y. Chen, X.K. Li, L. Meng, G. Liu, X. Ma, C. Piao, K. Wang, The fate and behavior

822   mechanism of antibiotic resistance genes and microbial communities in anaerobic

823   reactors treating oxytetracycline manufacturing wastewater, J. Hazard. Mater. 424

824   (2022) 127352. https://doi.org/10.1016/j.jhazmat.2021.127352.

825   [36]   S. Choi, J. Shin, K.J. Chae, Y.M. Kim, Mitigation via physiochemically enhanced primary

826   treatment of antibiotic resistance genes in influent from a municipal wastewater

827   treatment   plant,   Sep.   Purif.   Technol.   247   (2020)   116946.

828   https://doi.org/10.1016/j.seppur.2020.116946.

829   [37]   C. Liang, D. Wei, S. Zhang, Q. Ren, J. Shi, L. Liu, Removal of antibiotic resistance genes

830   from swine wastewater by membrane filtration treatment, Ecotoxicol. Environ. Saf. 210

831   (2021) 111885. https://doi.org/10.1016/j.ecoenv.2020.111885.

832   [38]   A. Thakur, N. Sharma, A. Mann, Removal of ofloxacin hydrochloride and paracetamol

833   from aqueous solutions: Binary mixtures and competitive adsorption, Mater. Today

834   Proc.   28   (2020)   1514–1519.

835   https://doi.org/https://doi.org/10.1016/j.matpr.2020.04.833.

836   [39]   A.H. Jawad, A.M. Kadhum, Y.S. Ngoh, Applicability of dragon fruit (Hylocereus

837   polyrhizus) peels as low-cost biosorbent for adsorption of methylene blue from

838   aqueous solution: Kinetics, equilibrium and thermodynamics studies, Desalin. Water

839   Treat. 109 (2018) 231–240. https://doi.org/10.5004/dwt.2018.21976.

840   [40]   D.S.P. Franco, J. Georgin, E.C. Lima, L.F.O. Silva, Journal of Water Process Engineering

841   Advances made in removing paraquat herbicide by adsorption technology : A review, J.

842   Water Process Eng. 49 (2022) 102988. https://doi.org/10.1016/j.jwpe.2022.102988.

843   [41]   J. Georgin, D.S.P. Franco, K. Da Boit Martinello, E.C. Lima, L.F.O. Silva, A review of the

844   toxicology presence and removal of ketoprofen through adsorption technology, J.

845   Environ. Chem. Eng. 10 (2022) 107798. https://doi.org/10.1016/j.jece.2022.107798.

846   [42]   P.S. Ghosal, A.K. Gupta, Determination of thermodynamic parameters from Langmuir

847 isotherm   constant-revisited,   J.   Mol.   Liq.   225   (2017)   137–146.
848 https://doi.org/10.1016/j.molliq.2016.11.058.

849 [43] N. Gupta, K. Poddar, D. Sarkar, N. Kumari, B. Padhan, A. Sarkar, Fruit waste
850 management by pigment production and utilization of residual as bioadsorbent, J.
851 Environ.   Manage.   244   (2019)   138–143.
852 https://doi.org/10.1016/j.jenvman.2019.05.055.

853 [44] K.Y. Foo, B.H. Hameed, Utilization of rice husk ash as novel adsorbent: A judicious
854 recycling of the colloidal agricultural waste, Adv. Colloid Interface Sci. 152 (2009) 39–
855 47. https://doi.org/10.1016/j.cis.2009.09.005.

856 [45] E. Worch, Fixed-bed adsorption in drinking water treatment: A critical review on models
857 and parameter estimation, J. Water Supply Res. Technol. 57 (2008) 171–183.
858 https://doi.org/10.2166/aqua.2008.100.

859 [46] P. Ma, Q. Liu, P. Liu, H. Li, X. Han, L. Liu, W. Zou, Green synthesis of Fe/Cu oxides
860 composite particles stabilized by pine needle extract and investigation of their
861 adsorption activity for norfloxacin and ofloxacin, J. Dispers. Sci. Technol. 42 (2021)
862 1350–1367. https://doi.org/10.1080/01932691.2020.1764367.

863 [47] L. Akhtar, M. Ahmad, S. Iqbal, A.A. Abdelhafez, M.T. Mehran, Biochars' adsorption
864 performance towards moxifloxacin and ofloxacin in aqueous solution: Role of pyrolysis
865 temperature and biomass type, Environ. Technol. Innov. 24 (2021) 101912.
866 https://doi.org/10.1016/j.eti.2021.101912.

867 [48] Y. Liu, Y. Yuan, Z. Wang, Y. Wen, L. Liu, T. Wang, X. Xie, Removal of ofloxacin from water
868 by natural ilmenite-biochar composite: A study on the synergistic adsorption
869 mechanism of multiple effects, Bioresour. Technol. 363 (2022) 127938.
870 https://doi.org/10.1016/j.biortech.2022.127938.

871 [49] N. Dhiman, Analysis of non-competitive and competitive adsorption behaviour of
872 ciprofloxacin hydrochloride and ofloxacin hydrochloride from aqueous solution using
873 oryza sativa husk ash (single and binary adsorption of antibiotics), Clean. Mater. 5
874 (2022) 100108. https://doi.org/10.1016/j.clema.2022.100108.

875 [50] N. Rueangchai, P. Noisong, S. Sansuk, A facile synthesis of hydroxyapatite and
876 hydroxyapatite/activated carbon composite for paracetamol and ofloxacin removal,
877 Mater.   Today   Commun.   34   (2023)   105326.
878 https://doi.org/10.1016/j.mtcomm.2023.105326.

879 [51] M. Sturini, C. Puscalau, G. Guerra, F. Maraschi, G. Bruni, F. Monteforte, A. Profumo, D.
880   Capsoni, Combined layer-by-layer/hydrothermal synthesis of fe3o4@mil-100(Fe) for
881   ofloxacin adsorption from environmental waters, Nanomaterials. 11 (2021).
882   https://doi.org/10.3390/nano11123275.

883 [52] R. Yu, Z. Wu, The adsorption property of in-situ synthesis of MOF in alginate gel for
884   ofloxacin in the wastewater, Environ. Technol. (United Kingdom). (2022) 1–12.
885   https://doi.org/10.1080/09593330.2022.2029579.

886 [53] S. He, Q. Chen, G. Chen, G. Shi, C. Ruan, M. Feng, Y. Ma, X. Jin, X. Liu, C. Du, C. He, H.
887   Dai, C. Cao, N-doped activated carbon for high-efficiency ofloxacin adsorption,
888   Microporous   Mesoporous   Mater.   335   (2022)   111848.
889   https://doi.org/10.1016/j.micromeso.2022.111848.

890 [54] R. Yu, Z. Wu, High adsorption for ofloxacin and reusability by the use of ZIF-8 for
891   wastewater treatment, Microporous Mesoporous Mater. 308 (2020) 110494.
892   https://doi.org/10.1016/j.micromeso.2020.110494.

893 [55] N.S. Sulaiman, M.H. Mohamad Amini, M. Danish, O. Sulaiman, R. Hashim, S. Demirel,
894   G.K. Demirel, Characterization and Ofloxacin Adsorption Studies of Chemically Modified
895   Activated   Carbon   from   Cassava   Stem,   Materials   (Basel).   15   (2022).
896   https://doi.org/10.3390/ma15155117.

897 [56] R. Antonelli, F.R. Martins, G.R.P. Malpass, M.G.C. da Silva, M.G.A. Vieira, Ofloxacin
898   adsorption by calcined Verde-lodo bentonite clay: Batch and fixed bed system
899   evaluation,   J.   Mol.   Liq.   315   (2020)   113718.
900   https://doi.org/10.1016/j.molliq.2020.113718.

901 [57] A. Jaswal, M. Kaur, S. Singh, S.K. Kansal, A. Umar, C.S. Garoufalis, S. Baskoutas,
902   Adsorptive removal of antibiotic ofloxacin in aqueous phase using rGO-MoS2
903   heterostructure,   J.   Hazard.   Mater.   417   (2021)   125982.
904   https://doi.org/10.1016/j.jhazmat.2021.125982.

905 [58] J. Hao, L. Wu, X. Lu, Y. Zeng, B. Jia, T. Luo, S. He, L. Liang, A stable Fe/Co bimetallic
906   modified biochar for ofloxacin removal from water: adsorption behavior and
907   mechanisms, RSC Adv. 12 (2022) 31650–31662. https://doi.org/10.1039/d2ra05334a.

908 [59] M. Ye, Y. Fang, H. Xiang, H. Liu, H. Yan, B. Wang, X. Lin, J. Liang, W. Qian, Preparation
909   and modification of bagasse biochar unveiling ofloxacin wastewater adsorption,
910   Environ.   Technol.   (United   Kingdom).   0   (2022)   1–12.

911   https://doi.org/10.1080/09593330.2022.2152222.

912   [60]   P. Verma, T. Das, P. Kumar, S. Das, Surface-passivated rGO@CuO/6A5N2TU colloidal

913   heterostructures for efficient removal of ofloxacin from contaminated water through

914   dual-mode complexation: insights into kinetics and adsorption isotherm model study,

915   Appl. Nanosci. (2022). https://doi.org/10.1007/s13204-022-02736-8.

916   [61]   V. Singh, V.C. Srivastava, Transformation of textile dyeing industrial sludge into

917   economical biochar for sorption of ofloxacin: equilibrium, kinetic, and cost analysis,

918   Biomass Convers. Biorefinery. (2022). https://doi.org/10.1007/s13399-022-02554-6.

919   [62]   P. Awasthi, R.S. Bangari, N. Sinha, PVDF / BNNSs nanocomposite membrane for

920   simultaneous removal of Tetracycline and Ofloxacin from water, J. Mol. Liq. 370 (2023)

921   120970. https://doi.org/10.1016/j.molliq.2022.120970.

922   [63]   B. Gao, Q. Chang, H. Yang, Selective adsorption of ofloxacin and ciprofloxacin from a

923   binary system using lignin-based adsorbents: Quantitative analysis, adsorption

924   mechanisms, and structure-activity relationship, Sci. Total Environ. 765 (2021) 144427.

925   https://doi.org/10.1016/j.scitotenv.2020.144427.

926   [64]   Y. Yang, Z. Zhong, J. Li, H. Du, Z. Li, Efficient with low-cost removal and adsorption

927   mechanisms of norfloxacin, ciprofloxacin, and ofloxacin on modified thermal kaolin:

928   experimental and theoretical studies, J. Hazard. Mater. 430 (2022) 128500.

929   https://doi.org/10.1016/j.jhazmat.2022.128500.

930   [65]   X. Qin, X. Zhong, B. Wang, G. Wang, F. Liu, L. Weng, Fractionation of levofloxacin and

931   ofloxacin during their transport in NOM-goethite: Batch and column studies, Environ.

932   Pollut. 316 (2023) 120542. https://doi.org/10.1016/j.envpol.2022.120542.

933   [66]   N. Le-Minh, S.J. Khan, J.E. Drewes, R.M. Stuetz, Fate of antibiotics during municipal

934   water recycling treatment processes, Water Res. 44 (2010) 4295–4323.

935   https://doi.org/10.1016/j.watres.2010.06.020.

936   [67]   D. Cheng, X. Liu, S. Zhao, B. Cui, J. Bai, Z. Li, Influence of the natural colloids on the multi-

937   phase distributions of antibiotics in the surface water from the largest lake in North

938   China, Sci. Total Environ. 578 (2017) 649–659.

939   https://doi.org/10.1016/j.scitotenv.2016.11.012.

940   [68]   J.B. Carbajo, A.L. Petre, R. Rosal, S. Herrera, P. Letón, E. García-Calvo, A.R. Fernández-

941   Alba, J.A. Perdigón-Melón, Continuous ozonation treatment of ofloxacin:

942   Transformation products, water matrix effect and aquatic toxicity, J. Hazard. Mater. 292

943   (2015) 34–43. https://doi.org/10.1016/j.jhazmat.2015.02.075.

944   [69]   M. Ashfaq, K.N. Khan, S. Rasool, G. Mustafa, M. Saif-Ur-Rehman, M.F. Nazar, Q. Sun,

945   C.P. Yu, Occurrence and ecological risk assessment of fluoroquinolone antibiotics in

946   hospital waste of Lahore, Pakistan, Environ. Toxicol. Pharmacol. 42 (2016) 16–22.

947   https://doi.org/10.1016/j.etap.2015.12.015.

948   [70]   P. Chen, L. Blaney, G. Cagnetta, J. Huang, B. Wang, Y. Wang, S. Deng, G. Yu, Degradation

949   of Ofloxacin by Perylene Diimide Supramolecular Nanofiber Sunlight-Driven

950   Photocatalysis, Environ. Sci. Technol. 53 (2019) 1564–1575.

951   https://doi.org/10.1021/acs.est.8b05827.

952   [71]   P.K. Cherukuri, P. Songkiatisak, F. Ding, J.M. Jault, X.H.N. Xu, Antibiotic Drug

953   Nanocarriers for Probing of Multidrug ABC Membrane Transporter of Bacillus subtilis,

954   ACS Omega. 5 (2020) 1625–1633. https://doi.org/10.1021/acsomega.9b03698.

955   [72]   P. Sharma, N. Kumar, R. Chauhan, V. Singh, V.C. Srivastava, R. Bhatnagar, Growth of

956   hierarchical ZnO nano flower on large functionalized rGO sheet for superior

957   photocatalytic mineralization of antibiotic, Chem. Eng. J. 392 (2020) 123746.

958   https://doi.org/10.1016/j.cej.2019.123746.

959   [73]   X. Chang, M.T. Meyer, X. Liu, Q. Zhao, H. Chen, J. an Chen, Z. Qiu, L. Yang, J. Cao, W.

960   Shu, Determination of antibiotics in sewage from hospitals, nursery, and

961   slaughterhouse, wastewater treatment plant and source water in Chongqing region of

962   Three Gorge Reservoir in China, Environ. Pollut. 158 (2010) 1444–1450.

963   https://doi.org/10.1016/j.envpol.2009.12.034.

964   [74]   P. Kovalakova, L. Cizmas, T.J. McDonald, B. Marsalek, M. Feng, V.K. Sharma, Occurrence

965   and toxicity of antibiotics in the aquatic environment: A review, Chemosphere. 251

966   (2020) 126351. https://doi.org/10.1016/j.chemosphere.2020.126351.

967   [75]   M.J. Fernandes, P. Paíga, A. Silva, C.P. Llaguno, M. Carvalho, F.M. Vázquez, C. Delerue-

968   Matos, Antibiotics and antidepressants occurrence in surface waters and sediments

969   collected in the north of Portugal, Chemosphere. 239 (2020).

970   https://doi.org/10.1016/j.chemosphere.2019.124729.

971   [76]   R. Andreozzi, R. Marotta, N. Paxéus, Pharmaceuticals in STP effluents and their solar

972   photodegradation in the aquatic environment, Chemosphere. 50 (2003) 1319–1330.

973   https://doi.org/10.1016/S0045-6535(02)00769-5.

974   [77]   H. Nakata, K. Kannan, P.D. Jones, J.P. Giesy, Determination of fluoroquinolone

antibiotics in wastewater effluents by liquid chromatography-mass spectrometry and fluorescence detection, Chemosphere. 58 (2005) 759–766. https://doi.org/10.1016/j.chemosphere.2004.08.097.

[78] D.G.J. Larsson, C. de Pedro, N. Paxeus, Effluent from drug manufacturers contains extremely high levels of pharmaceuticals, J. Hazard. Mater. 148 (2007) 751–755. https://doi.org/10.1016/j.jhazmat.2007.07.008.

[79] D. Quoc Tuc, M.G. Elodie, L. Pierre, A. Fabrice, T. Marie-Jeanne, B. Martine, E. Joelle, C. Marc, Fate of antibiotics from the hospital and domestic sources in a sewage network, Sci. Total Environ. 575 (2017) 758–766. https://doi.org/10.1016/j.scitotenv.2016.09.118.

[80] X. Yang, R.C. Flowers, H.S. Weinberg, P.C. Singer, Occurrence and removal of pharmaceuticals and personal care products (PPCPs) in an advanced wastewater reclamation plant, Water Res. 45 (2011) 5218–5228. https://doi.org/10.1016/j.watres.2011.07.026.

[81] H. Chen, L. Jing, Y. Teng, J. Wang, Characterization of antibiotics in a large-scale river system of China: Occurrence pattern, spatiotemporal distribution, and environmental risks, Sci. Total Environ. 618 (2018) 409–418. https://doi.org/10.1016/j.scitotenv.2017.11.054.

[82] M. Camotti Bastos, D. Rheinheimer dos Santos, É. Aubertheau, J.A.M. de Castro Lima, T. Le Guet, L. Caner, L. Mondamert, J. Labanowski, Antibiotics and microbial resistance in Brazilian soils under manure application, L. Degrad. Dev. 29 (2018) 2472–2484. https://doi.org/10.1002/ldr.2964.

[83] L.J. Zhou, G.G. Ying, J.L. Zhao, J.F. Yang, L. Wang, B. Yang, S. Liu, Trends in the occurrence of human and veterinary antibiotics in the sediments of the Yellow River, Hai River and Liao River in northern China, Environ. Pollut. 159 (2011) 1877–1885. https://doi.org/10.1016/j.envpol.2011.03.034.

[84] M.H. Wu, C.J. Que, G. Xu, Y.F. Sun, J. Ma, H. Xu, R. Sun, L. Tang, Occurrence, fate and interrelation of selected antibiotics in sewage treatment plants and their receiving surface water, Ecotoxicol. Environ. Saf. 132 (2016) 132–139. https://doi.org/10.1016/j.ecoenv.2016.06.006.

[85] B. Zhang, X. Han, P. Gu, S. Fang, J. Bai, Response surface methodology approach for optimization of ciprofloxacin adsorption using activated carbon derived from the

1007 residue of desilicated rice husk, J. Mol. Liq. 238 (2017) 316–325.
1008 https://doi.org/10.1016/j.molliq.2017.04.022.

1009 [86] D.N.D. Samaraweera, X. Liu, G. Zhong, T. Priyadarshana, R. Naseem Malik, G. Zhang,
1010 M.S. Khorram, Z. Zhu, X. Peng, Antibiotics in two municipal sewage treatment plants in
1011 Sri Lanka: Occurrence, consumption and removal efficiency, Emerg. Contam. 5 (2019)
1012 272–278. https://doi.org/10.1016/j.emcon.2019.08.001.

1013 [87] S. Aydin, M.E. Aydin, A. Ulvi, H. Kilic, Antibiotics in hospital effluents: occurrence,
1014 contribution to urban wastewater, removal in a wastewater treatment plant, and
1015 environmental risk assessment, Environ. Sci. Pollut. Res. 26 (2019) 544–558.
1016 https://doi.org/10.1007/s11356-018-3563-0.

1017 [88] Q. Bu, B. Wang, J. Huang, S. Deng, G. Yu, Pharmaceuticals and personal care products
1018 in the aquatic environment in China: A review, J. Hazard. Mater. 262 (2013) 189–211.
1019 https://doi.org/10.1016/j.jhazmat.2013.08.040.

1020 [89] L. Riaz, T. Mahmood, A. Khalid, A. Rashid, M.B. Ahmed Siddique, A. Kamal, M.S. Coyne,
1021 Fluoroquinolones (FQs) in the environment: A review on their abundance, sorption, and
1022 toxicity in soil, Chemosphere. 191 (2018) 704–720.
1023 https://doi.org/10.1016/j.chemosphere.2017.10.092.

1024 [90] A.Y.C. Lin, T.H. Yu, C.F. Lin, Pharmaceutical contamination in residential, industrial, and
1025 agricultural waste streams: Risk to aqueous environments in Taiwan, Chemosphere. 74
1026 (2008) 131–141. https://doi.org/10.1016/j.chemosphere.2008.08.027.

1027 [91] N.H. Tran, L. Hoang, L.D. Nghiem, N.M.H. Nguyen, H.H. Ngo, W. Guo, Q.T. Trinh, N.H.
1028 Mai, H. Chen, D.D. Nguyen, T.T. Ta, K.Y.H. Gin, Occurrence and risk assessment of
1029 multiple classes of antibiotics in urban canals and lakes in Hanoi, Vietnam, Sci. Total
1030 Environ. 692 (2019) 157–174. https://doi.org/10.1016/j.scitotenv.2019.07.092.

1031 [92] P. Guerra, M. Kim, A. Shah, M. Alaee, S.A. Smyth, Occurrence and fate of antibiotic,
1032 analgesic/anti-inflammatory, and antifungal compounds in five wastewater treatment
1033 processes, Sci. Total Environ. 473–474 (2014) 235–243.
1034 https://doi.org/10.1016/j.scitotenv.2013.12.008.

1035 [93] T.B. Minh, H.W. Leung, I.H. Loi, W.H. Chan, M.K. So, J.Q. Mao, D. Choi, J.C.W. Lam, G.
1036 Zheng, M. Martin, J.H.W. Lee, P.K.S. Lam, B.J. Richardson, Antibiotics in the Hong Kong
1037 metropolitan area: Ubiquitous distribution and fate in Victoria Harbour, Mar. Pollut.
1038 Bull. 58 (2009) 1052–1062. https://doi.org/10.1016/j.marpolbul.2009.02.004.

[94] H. Kim, Y.S. Hwang, V.K. Sharma, Adsorption of antibiotics and iopromide onto single-walled and multi-walled carbon nanotubes, Chem. Eng. J. 255 (2014) 23–27. https://doi.org/10.1016/j.cej.2014.06.035.

[95] A. Hartmann, A.C. Alder, T. Koller, R.M. Widmer, Identification of fluoroquinolone antibiotics as the main source of umuC genotoxicity in native hospital wastewater, Environ. Toxicol. Chem. 17 (1998) 377–382. https://doi.org/10.1897/1551-5028(1998)017<0377:IOFAAT>2.3.CO;2.

[96] D.M. Gattey, Toxicology, Garner Klintworth's Pathobiol. Ocul. Dis. Part B, Third Ed. (2007) 1079–1090. https://doi.org/10.5005/jp/books/14224_17.

[97] M. Rusch, A. Spielmeyer, H. Zorn, G. Hamscher, Degradation and transformation of fluoroquinolones by microorganisms with special emphasis on ciprofloxacin, Appl. Microbiol. Biotechnol. 103 (2019) 6933–6948. https://doi.org/10.1007/s00253-019-10017-8.

[98] K.Q. Xiao, B. Li, L. Ma, P. Bao, X. Zhou, T. Zhang, Y.G. Zhu, Metagenomic profiles of antibiotic resistance genes in paddy soils from South China, FEMS Microbiol. Ecol. 92 (2016). https://doi.org/10.1093/femsec/fiw023.

[99] H. Gao, F. Zhao, R. Li, S. Jin, H. Zhang, K. Zhang, S. Li, Q. Shu, G. Na, Occurrence and distribution of antibiotics and antibiotic resistance genes in the water of Liaohe River Basin, China, J. Environ. Chem. Eng. 10 (2022) 108297. https://doi.org/10.1016/j.jece.2022.108297.

[100] T.D. Nguyen, T. Itayama, R. Ramaraj, N. Iwami, K. Shimizu, T.S. Dao, T.L. Pham, H. Maseda, Chronic ecotoxicology and statistical investigation of ciprofloxacin and ofloxacin to Daphnia magna under extendedly long-term exposure, Environ. Pollut. 291 (2021) 118095. https://doi.org/10.1016/j.envpol.2021.118095.

[101] T.D. Nguyen, T. Itayama, R. Ramaraj, N. Iwami, K. Shimizu, T.S. Dao, T.L. Pham, H. Maseda, Physiological response of Simocephalus vetulus to five antibiotics and their mixture under 48-h acute exposure, Sci. Total Environ. 829 (2022) 154585. https://doi.org/10.1016/j.scitotenv.2022.154585.

[102] J. Xu, X. Liu, Y. Lv, X. Guo, S. Lu, Response of Cyperus involucratus to sulfamethoxazole and ofloxacin-contaminated environments: Growth physiology, transportation, and microbial community, Ecotoxicol. Environ. Saf. 206 (2020) 111332. https://doi.org/10.1016/j.ecoenv.2020.111332.

1071 [103] V. Singh, B. Pandey, S. Suthar, Phytotoxicity and degradation of antibiotic ofloxacin in
1072 duckweed (Spirodela polyrhiza) system, Ecotoxicol. Environ. Saf. 179 (2019) 88–95.
1073 https://doi.org/10.1016/j.ecoenv.2019.04.018.

1074 [104] M.I. Vasquez, M. Garcia-Käufer, E. Hapeshi, J. Menz, K. Kostarelos, D. Fatta-Kassinos, K.
1075 Kümmerer, Chronic ecotoxic effects to Pseudomonas putida and Vibrio fischeri, and
1076 cytostatic and genotoxic effects to the hepatoma cell line (HepG2) of ofloxacin
1077 photo(cata)lytically treated solutions, Sci. Total Environ. 450–451 (2013) 356–365.
1078 https://doi.org/10.1016/j.scitotenv.2012.05.096.

1079 [105] M. Kato, T. Onodera, Morphological investigation of cavity formation in articular
1080 cartilage induced by oiloxacin in rats, Toxicol. Sci. 11 (1988) 110–119.
1081 https://doi.org/10.1093/toxsci/11.1.110.

1082 [106] J.E. Burkhardt, M.A. Hill, W.W. Carlton, Morphologic and biochemical changes in
1083 articular cartilages of immature beagle dogs dosed with difloxacin, Toxicol. Pathol. 20
1084 (1992) 246–252. https://doi.org/10.1177/019262339202000211.

1085 [107] M. Machida, H. Kusajima, H. Aijima, A. Maeda, R. Ishida, H. Uchida, Toxicokinetic study
1086 of norfloxacin-induced arthropathy in juvenile animals, Toxicol. Appl. Pharmacol. 105
1087 (1990) 403–412. https://doi.org/10.1016/0041-008X(90)90144-J.

1088 [108] A.W. Gough, R.E. Sigler, Quinolone Arthropathy & mdash ; Acute Toxicity to Immature
1089 Articular Cartilage *, (n.d.) 436–449.

1090 [109] G. Corrao, A. Zambon, L. Bertù, A. Mauri, V. Paleari, C. Rossi, M. Venegoni, Evidence of
1091 tendinitis provoked by fluoroquinolone treatment a case-control study, Drug Saf. 29
1092 (2006) 889–896. https://doi.org/10.2165/00002018-200629100-00006.

1093 [110] L. Yang, M. Etminan, F.S. Mikelberg, Oral fluoroquinolones and risk of glaucoma, J.
1094 Glaucoma. 23 (2014) 464–466. https://doi.org/10.1097/IJG.0b013e31829463c1.

1095 [111] J.H.J. Droste, M.H. Wieringa, J.J. Weyler, V.J. Nelen, P.A. Vermeire, H.P. Van Bever, Does
1096 the use of antibiotics in early childhood increase the risk of asthma and allergic
1097 disease?, Clin. Exp. Allergy. 30 (2000) 1548–1553. https://doi.org/10.1046/j.1365-
1098 2222.2000.00939.x.

1099 [112] K.H. Mikkelsen, K.H. Allin, F.K. Knop, Effect of antibiotics on gut microbiota, glucose
1100 metabolism, and body weight regulation: A review of the literature, Diabetes, Obes.
1101 Metab. 18 (2016) 444–453. https://doi.org/10.1111/dom.12637.

1102 [113] J.S. Cohen, Peripheral neuropathy associated with fluoroquinolones, Ann.

1103   Pharmacother. 35 (2001) 1540–1547. https://doi.org/10.1345/aph.1Z429.

1104 [114] P.D. Cani, R. Bibiloni, C. Knauf, A.M. Neyrinck, N.M. Delzenne, Changes in gut microbiota

1105   control metabolic diet-induced obesity and diabetes in mice, Diabetes. 57 (2008) 1470–

1106   81. https://doi.org/10.2337/db07-1403.Additional.

1107 [115] S. Shao, W. Pan, B. Wang, Y. Liu, H. Gan, M. Li, T. Liao, X. Yang, Q. Yang, C. Huang, M.

1108   Geng, G. Pan, K. Liu, P. Zhu, F. Tao, Association between antibiotic exposure and the

1109   risk of infertility in women of childbearing age: A case-control study, Ecotoxicol.

1110   Environ. Saf. 249 (2023) 114414. https://doi.org/10.1016/j.ecoenv.2022.114414.

1111 [116] J. Zhang, Z. Liu, S. Song, J. Fang, L. Wang, L. Zhao, C. Li, W. Li, H.M. Byun, L. Guo, P. Li,

1112   The exposure levels and health risk assessment of antibiotics in urine and its association

1113   with platelet mitochondrial DNA methylation in adults from Tianjin, China: A

1114   preliminary study, Ecotoxicol. Environ. Saf. 231 (2022) 113204.

1115   https://doi.org/10.1016/j.ecoenv.2022.113204.

1116 [117] Z.G. Sheng, W. Huang, Y.X. Liu, Y. Yuan, B.Z. Zhu, Ofloxacin induces apoptosis via $\beta 1$

1117   integrin-EGFR-Rac1-Nox2 pathway in microencapsulated chondrocytes, Toxicol. Appl.

1118   Pharmacol. 267 (2013) 74–87. https://doi.org/10.1016/j.taap.2012.12.015.

1119 [118] D.S.P. Franco, J.L.S. Fagundes, J. Georgin, N.P.G. Salau, G.L. Dotto, A mass transfer study

1120   considering intraparticle diffusion and axial dispersion for fixed-bed adsorption of

1121   crystal violet on pecan pericarp (Carya illinoensis), Chem. Eng. J. 397 (2020) 125423.

1122   https://doi.org/10.1016/j.cej.2020.125423.

1123 [119] A. Bonilla-Petriciolet, D.I. Mendoza-Castillo, G.L. Dotto, C.J. Duran-Valle, I.T. De

1124   Aguascalientes, Adsorption in Water Treatment, Elsevier Inc., 2019.

1125   https://doi.org/10.1016/B978-0-12-409547-2.14390-2.

1126 [120] I. Langmuir, The adsorption of gases on plane surfaces of glass, mica and platinum, J.

1127   Am. Chem. Soc. 40 (1918) 1361–1403. https://doi.org/10.1021/ja02242a004.

1128 [121] H.M.F. Freundlich, Over the adsorption in solution, J. Phys. Chem. 57 (1906) 358–471.

1129 [122] A.W. Marczewski, Analysis of kinetic langmuir model. Part I: Integrated kinetic langmuir

1130   equation (IKL): A new complete analytical solution of the langmuir rate equation,

1131   Langmuir. 26 (2010) 15229–15238. https://doi.org/10.1021/la1010049.

1132 [123] C.M. Kerkhoff, K. da Boit Martinello, D.S.P. Franco, M.S. Netto, J. Georgin, E.L. Foletto,

1133   D.G.A. Piccilli, L.F.O. Silva, G.L. Dotto, Adsorption of ketoprofen and paracetamol and

1134   treatment of a synthetic mixture by novel porous carbon derived from Butia capitata

1135 endocarp, J. Mol. Liq. 339 (2021) 117184.
1136 https://doi.org/10.1016/j.molliq.2021.117184.

1137 [124] J. Georgin, D.S.P. Franco, M.S. Netto, M.S. Manzar, M. Zubair, L. Meili, D.G.A. Piccilli,
1138 L.F.O. Silva, Adsorption of the First-Line Covid Treatment Analgesic onto Activated
1139 Carbon from Residual Pods of Erythrina Speciosa, Environ. Manage. 2019 (2022).
1140 https://doi.org/10.1007/s00267-022-01716-6.

1141 [125] D.S.P. Franco, J. Georgin, M.S. Netto, K. da Boit Martinello, L.F.O. Silva, Preparation of
1142 activated carbons from fruit residues for the removal of naproxen (NPX): Analytical
1143 interpretation via statistical physical model, J. Mol. Liq. 356 (2022) 119021.
1144 https://doi.org/10.1016/j.molliq.2022.119021.

1145 [126] J.O. Ighalo, C.A. Igwegbe, A.G. Adeniyi, C.A. Adeyanju, S. Ogunniyi, Mitigation of
1146 Metronidazole (Flagyl) pollution in aqueous media by adsorption: a review, Environ.
1147 Technol. Rev. 9 (2020) 137–148. https://doi.org/10.1080/21622515.2020.1849409.

1148 [127] S. Iftekhar, D.L. Ramasamy, V. Srivastava, M.B. Asif, M. Sillanpää, Understanding the
1149 factors affecting the adsorption of Lanthanum using different adsorbents: A critical
1150 review, Chemosphere. 204 (2018) 413–430.
1151 https://doi.org/10.1016/J.CHEMOSPHERE.2018.04.053.

1152 [128] J. Lyklema, Points of zero charge in the presence of specific adsorption, J. Colloid
1153 Interface Sci. 99 (1984) 109–117. https://doi.org/10.1016/0021-9797(84)90090-0.

1154 [129] G. Kaur, N. Singh, A. Rajor, J.P. Kushwaha, Deep eutectic solvent functionalized rice husk
1155 ash for effective adsorption of ofloxacin from aqueous environment, J. Contam. Hydrol.
1156 242 (2021) 103847. https://doi.org/10.1016/j.jconhyd.2021.103847.

1157 [130] R.S. Bangari, N. Sinha, Adsorption of tetracycline, ofloxacin and cephalexin antibiotics
1158 on boron nitride nanosheets from aqueous solution, J. Mol. Liq. 293 (2019) 111376.
1159 https://doi.org/10.1016/j.molliq.2019.111376.

1160 [131] M. Thakur, A. Sharma, V. Ahlawat, M. Bhattacharya, S. Goswami, Process optimization
1161 for the production of cellulose nanocrystals from rice straw derived α-cellulose, Mater.
1162 Sci. Energy Technol. 3 (2020) 328–334. https://doi.org/10.1016/j.mset.2019.12.005.

1163 [132] C. Zhu, Y. Lang, B. Liu, H. Zhao, Ofloxacin Adsorption on Chitosan/Biochar Composite:
1164 Kinetics, Isotherms, and Effects of Solution Chemistry, Polycycl. Aromat. Compd. 39
1165 (2019) 287–297. https://doi.org/10.1080/10406638.2018.1464039.

1166 [133] Z.H. Hu, Y.F. Wang, A.M. Omer, X.K. Ouyang, Fabrication of ofloxacin imprinted polymer

on the surface of magnetic carboxylated cellulose nanocrystals for highly selective adsorption of fluoroquinolones from water, Int. J. Biol. Macromol. 107 (2018) 453–462. https://doi.org/10.1016/j.ijbiomac.2017.09.009.

[134] B. Gao, P. Li, R. Yang, A. Li, H. Yang, Investigation of multiple adsorption mechanisms for efficient removal of ofloxacin from water using lignin-based adsorbents, Sci. Rep. 9 (2019) 1–13. https://doi.org/10.1038/s41598-018-37206-1.

[135] C.L. Zhang, F. Zhao, Y. Wang, Thermodynamic and kinetic parameters of ofloxacin adsorption from aqueous solution onto modified coal fly ash, Russ. J. Phys. Chem. A. 86 (2012) 653–657. https://doi.org/10.1134/S0036024412040346.

[136] J. Ma, N. Yan, M. Zhang, J. Liu, X. Bai, Y. Wang, Mechanical characteristics of soda residue soil incorporating different admixture: Reuse of soda residue, Sustain. 12 (2020). https://doi.org/10.3390/su12145852.

[137] J. Georgin, D.S.P. Franco, F.C. Drumm, P. Grassi, M. Schadeck Netto, D. Allasia, G.L. Dotto, Paddle cactus (Tacinga palmadora) as potential low-cost adsorbent to treat textile effluents containing crystal violet, Chem. Eng. Commun. 207 (2020) 1368–1379. https://doi.org/10.1080/00986445.2019.1650033.

[138] D.S.P. Franco, J. Georgin, F.C. Drumm, M.S. Netto, D. Allasia, M.L.S. Oliveira, G.L. Dotto, Araticum (Annona crassiflora) seed powder (ASP) for the treatment of colored effluents by biosorption, Environ. Sci. Pollut. Res. 27 (2020) 11184–11194. https://doi.org/10.1007/s11356-019-07490-z.

[139] É.C. Lima, M.H. Dehghani, A. Guleria, F. Sher, R.R. Karri, G.L. Dotto, H.N. Tran, Adsorption: Fundamental aspects and applications of adsorption for effluent treatment, in: M. Hadi Dehghani, R. Karri, E. Lima (Eds.), Green Technol. Defluoridation Water, Elsevier, 2021: pp. 41–88. https://doi.org/10.1016/b978-0-323-85768-0.00004-x.

[140] K.Y. Foo, B.H. Hameed, Potential of jackfruit peel as a precursor for activated carbon prepared by microwave-induced NaOH activation, Bioresour. Technol. 112 (2012) 143–150. https://doi.org/10.1016/j.biortech.2012.01.178.

[141] A.M. Awad, S.M.R. Shaikh, R. Jalab, M.H. Gulied, M.S. Nasser, A. Benamor, S. Adham, Adsorption of organic pollutants by natural and modified clays: A comprehensive review, Sep. Purif. Technol. 228 (2019) 115719. https://doi.org/10.1016/j.seppur.2019.115719.

[142] O.S. Bello, K.A. Adegoke, O.O. Sarumi, O.S. Lameed, Functionalized locust bean pod (Parkia biglobosa) activated carbon for Rhodamine B dye removal, Heliyon. 5 (2019) e02323. https://doi.org/10.1016/j.heliyon.2019.e02323.

[143] G. Mckay, Use of adsorbents for the removal of pollutants from wastewaters, 1st ed., CRC Press, 1996.

[144] O. Redlich, D.L. Peterson, A Useful Adsorption Isotherm, J. Phys. Chem. 63 (1959) 1024–1024. https://doi.org/10.1021/j150576a611.

[145] E.C. Lima, A.A. Gomes, H.N. Tran, Comparison of the nonlinear and linear forms of the van't Hoff equation for calculation of adsorption thermodynamic parameters ($\Delta S°$ and $\Delta H°$), J. Mol. Liq. 311 (2020) 113315. https://doi.org/10.1016/j.molliq.2020.113315.

[146] A.J. Phares, F.J. Wunderlich, EFFECT OF ADSORBATE-ADSORBATE INTERACTIONS ON LOW-TEMPERATURE SURFACE ADSORPTION PATTERNS, Int. J. Mod. Phys. B. 15 (2012) 3323–3330. https://doi.org/10.1142/S0217979201007701.

[147] D.R. Lima, E.C. Lima, P.S. Thue, S.L.P. Dias, F.M. Machado, M.K. Seliem, F. Sher, G.S. dos Reis, M.R. Saeb, J. Rinklebe, Comparison of acidic leaching using a conventional and ultrasound-assisted method for preparation of magnetic-activated biochar, J. Environ. Chem. Eng. 9 (2021) 105865. https://doi.org/10.1016/j.jece.2021.105865.

[148] C.O. Aniagor, M.C. Menkiti, Kinetics and mechanistic description of adsorptive uptake of crystal violet dye by lignified elephant grass complexed isolate, J. Environ. Chem. Eng. 6 (2018) 2105–2118. https://doi.org/10.1016/j.jece.2018.01.070.

[149] C.O. Aniagor, C.A. Igwegbe, J.O. Ighalo, S.N. Oba, Adsorption of doxycycline from aqueous media: A review, J. Mol. Liq. 334 (2021) 116124. https://doi.org/10.1016/J.MOLLIQ.2021.116124.

[150] E.C. Lima, F. Sher, A. Guleria, M.R. Saeb, I. Anastopoulos, H.N. Tran, A. Hosseini-Bandegharaei, Is one performing the treatment data of adsorption kinetics correctly?, J. Environ. Chem. Eng. 9 (2021) 104813. https://doi.org/10.1016/j.jece.2020.104813.

[151] S. Sircar, Adsorbate mass transfer into porous adsorbents – A practical viewpoint, Sep. Purif. Technol. 192 (2018) 383–400. https://doi.org/10.1016/J.SEPPUR.2017.10.014.

[152] J. Georgin, Y.L. de O. Salomón, D.S.P.P. Franco, M.S. Netto, D.G.A. Piccilli, D. Perondi, L.F.O.O. Silva, E.L. Foletto, G.L. Dotto, G. Daniel, J. Georgin, Y.L.D.O. Salom, A. Piccilli, D. Perondi, L.F.O.O. Silva, E.L. Foletto, G.L. Dotto, Y.L. de O. Salomón, D.S.P.P. Franco, M.S. Netto, D.G.A. Piccilli, D. Perondi, L.F.O.O. Silva, E.L. Foletto, G.L. Dotto, Development of

highly porous activated carbon from Jacaranda mimosifolia seed pods for remarkable removal of aqueous-phase ketoprofen, J. Environ. Chem. Eng. 9 (2021) 105676. https://doi.org/10.1016/j.jece.2021.105676.

[153] J.O. Ighalo, O.J. Ajala, G. Umenweke, S. Ogunniyi, C.A. Adeyanju, C.A. Igwegbe, A.G. Adeniyi, Mitigation of clofibric acid pollution by adsorption: A review of recent developments, J. Environ. Chem. Eng. 8 (2020) 104264. https://doi.org/10.1016/j.jece.2020.104264.

[154] S. Li, K. Han, J. Li, M. Li, C. Lu, Preparation and characterization of super activated carbon produced from gulfweed by KOH activation, Microporous Mesoporous Mater. 243 (2017) 291–300. https://doi.org/10.1016/j.micromeso.2017.02.052.

[155] Y. Vieira, M.B. Ceretta, E.L. Foletto, E.A. Wolski, S. Silvestri, Application of a novel rGO-CuFeS2 composite catalyst conjugated to microwave irradiation for ultra-fast real textile wastewater treatment, J. Water Process Eng. 36 (2020) 101397. https://doi.org/10.1016/J.JWPE.2020.101397.

[156] M.B. Ceretta, Y. Vieira, E.A. Wolski, E.L. Foletto, S. Silvestri, Biological degradation coupled to photocatalysis by ZnO/polypyrrole composite for the treatment of real textile wastewater, J. Water Process Eng. 35 (2020) 101230. https://doi.org/10.1016/j.jwpe.2020.101230.

[157] G. Gupta, S.K. Kansal, A. Umar, S. Akbar, Visible-light driven excellent photocatalytic degradation of ofloxacin antibiotic using BiFeO3 nanoparticles, Chemosphere. 314 (2023) 137611. https://doi.org/10.1016/j.chemosphere.2022.137611.

[158] Q. Su, J. Li, H. Yuan, B. Wang, Y. Wang, Y. Li, Y. Xing, Visible-light-driven photocatalytic degradation of ofloxacin by g-C3N4/NH2-MIL-88B(Fe) heterostructure: Mechanisms, DFT calculation, degradation pathway, and toxicity evolution, Chem. Eng. J. 427 (2022). https://doi.org/10.1016/j.cej.2021.131594.

[159] S. Mandal, S. Adhikari, S. Choi, Y. Lee, D.H. Kim, Fabrication of a novel Z-scheme Bi2MoO6/GQDs/MoS2 hierarchical nanocomposite for the photo-oxidation of ofloxacin and photoreduction of Cr(VI) as aqueous pollutants, Chem. Eng. J. 444 (2022) 136609. https://doi.org/10.1016/j.cej.2022.136609.

[160] P. Xu, D. Zheng, Q. He, J. Yu, The feasibility of ofloxacin degradation and electricity generation in photo-assisted microbial fuel cells with LiNbO3/CF photocatalytic cathode, Sep. Purif. Technol. 250 (2020) 117106.

1263   https://doi.org/10.1016/j.seppur.2020.117106.

1264   [161] Z. Du, K. Li, S. Zhou, X. Liu, Y. Yu, Y. Zhang, Y. He, Y. Zhang, Degradation of ofloxacin with

1265   heterogeneous photo-Fenton catalyzed by biogenic Fe-Mn oxides, Chem. Eng. J. 380

1266   (2020) 122427. https://doi.org/10.1016/j.cej.2019.122427.

1267   [162] M. Taherizadeh, S. Jahani, M. Moradalizadeh, M.M. Foroughi, Synthesis of a dual-

1268   functional terbium doped copper oxide nanoflowers for high-efficiently

1269   electrochemical sensing of ofloxacin, pefloxacin and gatifloxacin, Talanta. 255 (2023)

1270   124216. https://doi.org/10.1016/j.talanta.2022.124216.

1271   [163] H. Chen, J. Wang, Degradation and mineralization of ofloxacin by ozonation and

1272   peroxone (O3/H2O2) process, Chemosphere. 269 (2021) 128775.

1273   https://doi.org/10.1016/j.chemosphere.2020.128775.

1274   [164] A. Mojiri, M. Vakili, H. Farraji, S.Q. Aziz, Combined ozone oxidation process and

1275   adsorption methods for the removal of acetaminophen and amoxicillin from aqueous

1276   solution; kinetic and optimisation, Environ. Technol. Innov. 15 (2019) 100404.

1277   https://doi.org/10.1016/j.eti.2019.100404.

1278   [165] J. Shadmehr, S.M. Mirsoleimani-Azizi, S. Zeinali, P. Setoodeh, Electrocoagulation

1279   process for propiconazole elimination from wastewater: experimental design for

1280   correlative modeling and optimization, Int. J. Environ. Sci. Technol. 16 (2019) 5409–

1281   5420. https://doi.org/10.1007/s13762-018-1891-8.

1282   [166] C. Thakur, V.C. Srivastava, I.D. Mall, Electrochemical treatment of distillery wastewater:

1283   Parametric and residue disposal study, Chem. Eng. J. 148 (2009) 496–505.

1284   https://doi.org/10.1016/j.cej.2008.09.043.

1285   [167] D.T. Moussa, M.H. El-Naas, M. Nasser, M.J. Al-Marri, A comprehensive review of

1286   electrocoagulation for water treatment: Potentials and challenges, J. Environ. Manage.

1287   186 (2017) 24–41. https://doi.org/10.1016/j.jenvman.2016.10.032.

1288   [168] I. Maldonado, E.G. Moreno Terrazas, F.Z. Vilca, Application of duckweed (Lemna sp.)

1289   and water fern (Azolla sp.) in the removal of pharmaceutical residues in water: State of

1290   the art focus on antibiotics, Sci. Total Environ. 838 (2022) 156565.

1291   https://doi.org/10.1016/j.scitotenv.2022.156565.

1292   [169] G. Akerman-Sanchez, K. Rojas-Jimenez, Fungi for the bioremediation of

1293   pharmaceutical-derived pollutants: A bioengineering approach to water treatment,

1294   Environ. Adv. 4 (2021) 100071. https://doi.org/10.1016/j.envadv.2021.100071.

1295   [170] M. Martínez-Ruiz, A. Molina-Vázquez, B. Santiesteban-Romero, H. Reyes-Pardo, K.R.
1296   Villaseñor-Zepeda, E.R. Meléndez-Sánchez, R.G. Araújo, J.E. Sosa-Hernández, M. Bilal,
1297   H.M.N. Iqbal, R. Parra-Saldivar, Micro-algae assisted green bioremediation of water
1298   pollutants rich leachate and source products recovery, Environ. Pollut. 306 (2022).
1299   https://doi.org/10.1016/j.envpol.2022.119422.

1300   [171] J. Georgin, D.S.P. Franco, M.S. Netto, B.M.V. Gama, D.P. Fernandes, P. Sepúlveda, L.F.O.
1301   Silva, L. Meili, Effective adsorption of harmful herbicide diuron onto novel activated
1302   carbon from Hovenia dulcis, Colloids Surfaces A Physicochem. Eng. Asp. 654 (2022)
1303   129900. https://doi.org/10.1016/j.colsurfa.2022.129900.

1304
1305

List of Figures
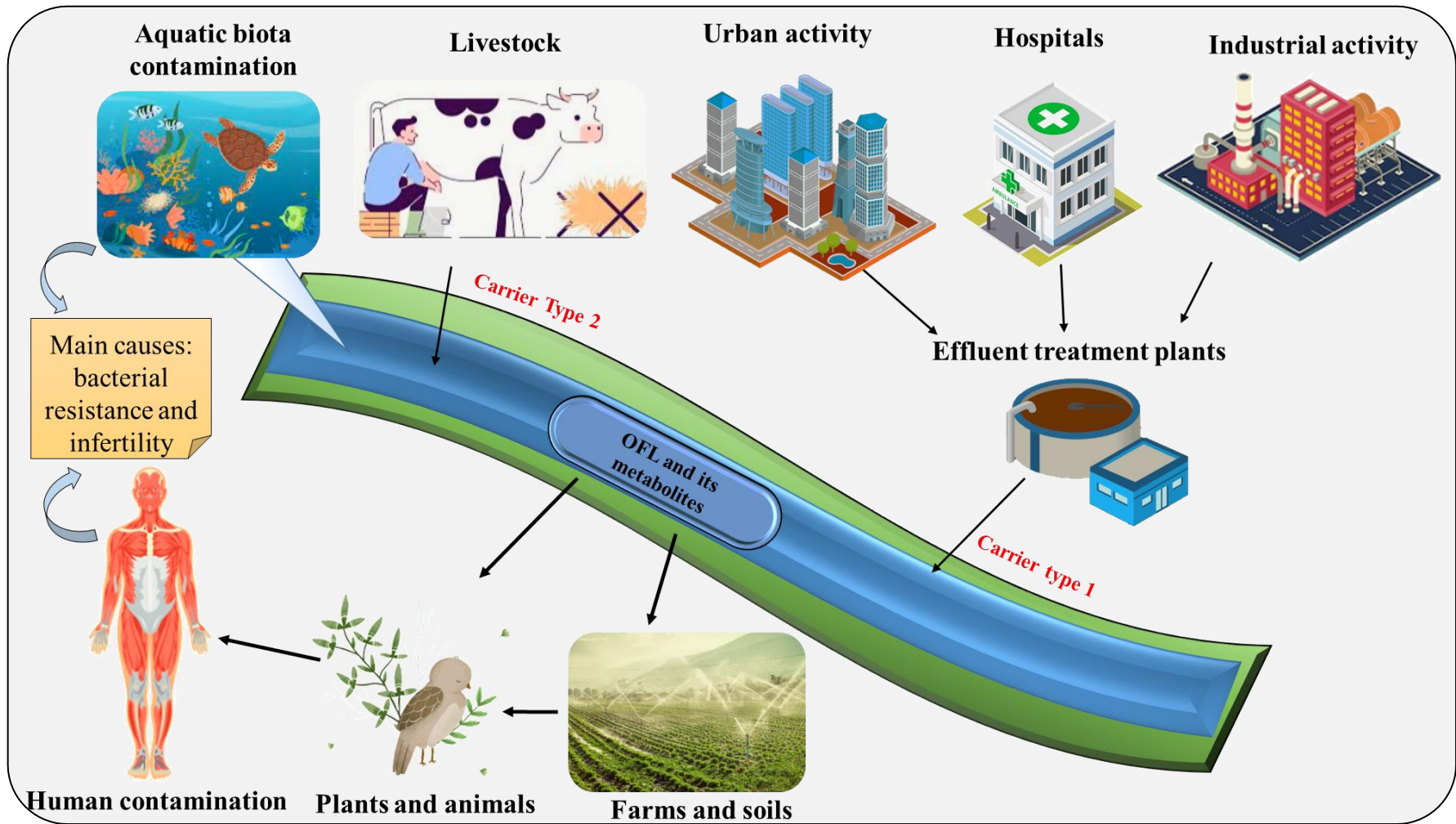
Figure 1: Mechanisms and sources of release of OFL in water resources.
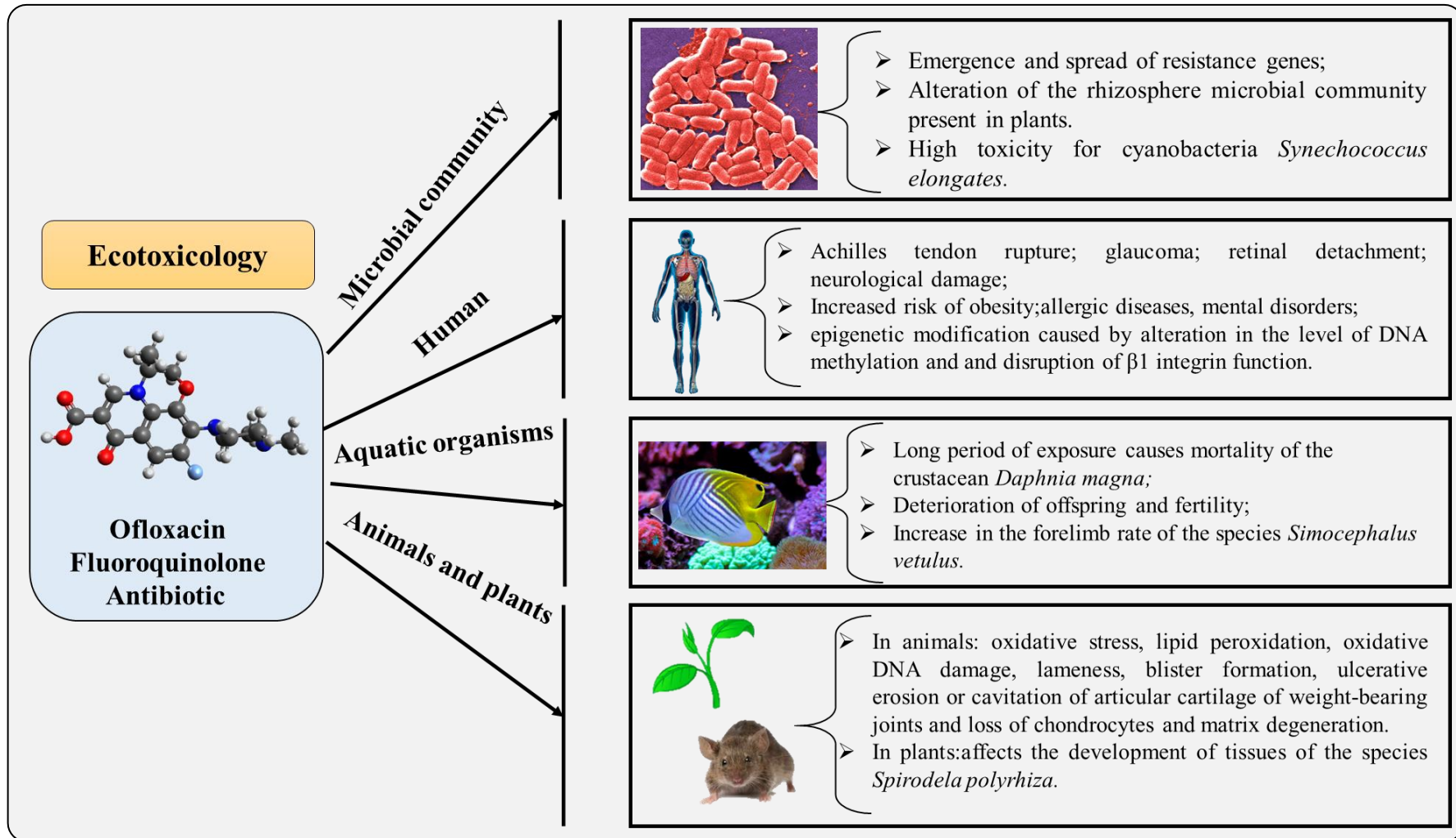
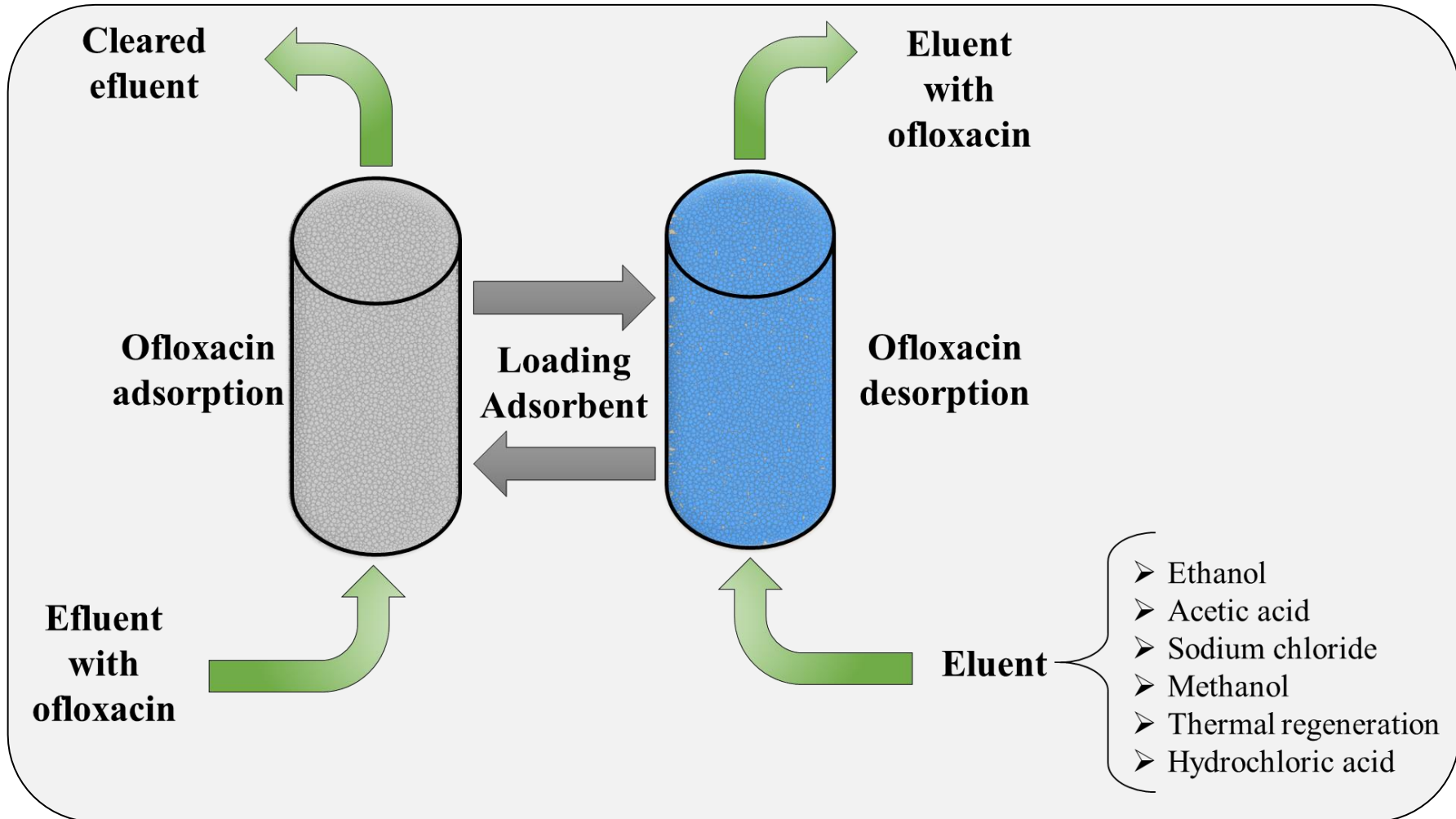**Figure 2:** Toxic effects of OFL at the human and environmental levels.

Figure 3: Desorption of OFL using different eluents used in the literature.